C. R. Physique 15 (2014) 158–175

Contents lists available at ScienceDirect

Comptes Rendus Physique

www.sciencedirect.com

Electron microscopy / Microscopie électronique

# Seeing and measuring in colours: Electron microscopy and spectroscopies applied to nano-optics

## *Voir et mesurer en couleur: microscopie et spectroscopies électroniques pour la nano-optique*

Mathieu Kociak, Odile Stéphan, Alexandre Gloter, Luiz F. Zagonel [1], Luiz H.G. Tizei, Marcel Tencé, Katia March, Jean Denis Blazit, Zackaria Mahfoud, Arthur Losquin, Sophie Meuret, Christian Colliex

*Laboratoire de physique des solides, CNRS UMR 8502, Université Paris-Sud, 91405 Orsay, France*

ARTICLE INFO

*Article history:*
Available online 27 January 2014

*Keywords:*
Scanning transmission electron microscopy
Electron energy loss spectroscopy
Cathodoluminescence
Surface plasmons
Excitons
Nano-optics

*Mots-clés :*
Microscopie électronique à transmission en balayage
Spectroscopie de perte d'énergie d'électrons
Cathodoluminescence
Plasmons de surface
Excitons
Nano-optique

ABSTRACT

Over the past ten years, Scanning Transmission Electron Microscopes (STEM) fitted with Electron Energy Loss Spectroscopy (EELS) and/or Cathodoluminescence (CL) spectroscopy have demonstrated to be essential tools for probing the optical properties of nano-objects at sub-wavelength scales. Thanks to the possibility of measuring them at a nanometer scale in parallel to the determination of the structure and morphology of the object of interest, new challenging experimental and theoretical horizons have been unveiled. As regards optical properties of metallic nanoparticles, surface plasmons have been mapped at a scale unimaginable only a few years ago, while the relationship between the energy levels and the size of semiconducting nanostructures a few atomic layers thick could directly be measured. This paper reviews some of these highly stimulating recent developments.



RÉSUMÉ

Au cours des dix années écoulées, les microscopes électroniques à transmission en balayage (STEM) equipés pour la spectroscopie de perte d'énergie d'électrons (EELS) et/ou la cathodoluminescence (CL) ont démontré leur capacité fondamentale pour une étude fine des propriétés optiques de nano-objets à l'échelle sub-longueur d'onde. Comme ils permettent de les mesurer au niveau du nanomètre en même temps que leur structure et morphologie au niveau atomique, de nouveaux champs d'étude aussi bien expérimentaux que théoriques ont ainsi pu être explorés. En ce qui concerne la réponse optique de nanoparticules métalliques, les plasmons de surface ont été cartographiés à une échelle qui aurait été inimaginable il y a encore quelques années, tandis que la relation entre les niveaux d'énergie et la taille de nanostructures semiconductrices épaisses de quelques couches atomiques a pu être directement établie. Cet article a pour but de présenter une revue rapide de quelques-uns des résultats récents les plus spectaculaires dans ce domaine.



[1] Now at: Instituto de Física Gleb Wataghin, Universidade Estadual de Campinas – UNICAMP, 13083-859 Campinas, SP, Brazil.

1631-0705/$ – see front matter 
http://dx.doi.org/10.1016/j.crhy.2013.10.003

## 1. Introduction

In recent years, the number of studies on the optical properties of nanoparticles or nanostructured materials has literally exploded. Most probably, this is due to the fact that these optical properties can be manipulated and designed at will by playing with the nanostructures sizes and shapes, and the skills and creativity of chemists and technologists have provided over the past years the physicist with an access to such on-purpose designed nano-objects.

Nowadays, the relevant scale can be as small as a nanometer for optical properties, and, since these are so dependent on the structure and morphology, these latter may have to be known with an atomic precision.

Indeed, many fundamental and more applied issues rely on the observation of optical properties at these scales. As an example, the behaviour of the light at distances much smaller than its wavelength is a fascinating and counterintuitive topic. Another example is the development of Light Emitting Diodes (LEDs), or the optimisation of photovoltaic devices, that heavily rely on the miniaturisation and nanostructuration of the materials they are made up of. It is thus an exciting challenge to explore and measure the optical properties variations of such important industrial devices at the relevant scale, i.e. over a few nanometers scale. Therefore, the fundamental limits of optical techniques relying on photons alone call for the introduction of disruptive methods and concepts, which have appeared these last years and which will be described in this review paper.

Needless to say, standard optical means—such as visible–UV spectroscopy or PhotoLuminescence, PL—, even in a confocal set-up, cannot go below the diffraction limit and can't address the issue efficiently. Stunning optical techniques, such as the STimulated Emission Depletion (STED), can now reach true nanometer resolution, optionally in 3D [1]. However, they are limited to specific applications, and cannot help at determining the structure or morphology of the objects of interest. Other alternatives, such as the PhotoEmission Electron Microscopy (PEEM) [2], despite their interest, have not yet demonstrated resolutions better than a few nanometers.

At the opposite, fast electron microscopies, such as Scanning (Transmission) Electron Microscopies—S(T)EM—, taking advantage of the very short de Broglie wavelength of accelerated electrons can produce nowadays sub-angström probes. They reveal the structure of nano-objects down to their atomic configuration. The optical properties can then be investigated in parallel through spectroscopic measurements.

However, before trying to understand how optical properties can be deduced from electron spectroscopies, let us remind that the notion of optical properties is not unique and that it depends on the way those properties are measured. In a traditional optical experiment, one sends a light beam on the sample of interest. Part of the light is scattered at the same energy, at a different one, or absorbed by the sample. This corresponds to the scattering, luminescence, or absorption optical properties. Finally, if after sending a light beam onto a sample, one observes the decrease of intensity along its path, one is dealing with the so-called extinction properties. All these properties, the measurement of which allows access to different information, are interconnected. The extinction cross section is the sum of the absorption, scattering and luminescence one.

How can we understand that an electron, which in free space would never interact with light, can help measuring optical properties? An heuristic point of view is as follows. A fast electron carries a Coulomb field. A nanoparticle close to the electron trajectory experiences a time-varying electric field pointing from the electron to the nanoparticle. When the electron is close to the nanoparticle, the interaction is strong and the electric field points roughly perpendicular to the electron trajectory, while when it is far, it is too weak to be relevant. Thus, the nanoparticle feels a pulse of electromagnetic radiation propagating along, and with an electrical field oriented mostly perpendicular to the electron axis. This resembles dramatically a plane wave packet of light propagating along the electron path. Since the pulse is relatively short in time (for a 10 nm thick nanoparticle and an electron travelling at half the speed of light, the interaction time is typically less than a fs), the spectrum of the electromagnetic field accompanying the electron is white. Furthermore, the field is concentrated on a very small volume (due to the localised Coulomb interaction it is made up of). One may then view the electron as a highly localised white source of light. In the following, it is this "light" which is absorbed, scattered or responsible for the luminescence phenomena—and not the electron itself!

Now, two different brands of spectroscopies are of interest when trying to unveil the optical properties of nano-objects with electrons. When a fast electron is sent onto or close to an object of interest, it can transfer some energy through Coulomb interaction. If one is able to measure the amount of energy lost by the electrons, one has access to the extinction properties of the object of interest. Luckily enough, such energy loss can be measured through Electron Energy Loss Spectroscopy (EELS), which is here intuitively cast as an extinction spectroscopy at the nanometer scale.

Of course, the energy transferred to the object has to be released. If by chance this happens in the form of a photon in the Infra Red/visible/Ultra Violet (IR/VIS/UV) range, then one have access to the luminescence or scattering properties through the so-called Cathodoluminescence (CL) spectroscopy.

The fact that both techniques can really reveal these properties at a few nanometers scale or less, is not straightforward as it implies both conceptual and technical issues. These issues have nowadays been partly solved, and have led to an impressive amount of work, both experimental and theoretical, and to conceptual advances in the study of plasmons in metallic nano-objects (through EELS and in a lesser extent CL) and of excitons in semiconducting structures (by CL). A comprehensive and excellent review, mainly devoted to plasmon and photonics excitations has been recently published [3]. This reference is a must for all those who aim at a deep understanding of the physics behind optical excitations at the nanometer level and how electrons can be used to explore them. However, since this publication, the field has kept growing very quickly and this is the intent of this paper to review these recent advances.

## 2. Principle

### 2.1. EELS and CL generalities

In an EELS experiment, a fast electron beam is sent onto the sample of interest, and the inelastically scattered electrons are sent to a scintillator after having been dispersed in energy through a magnetic prism. The EELS spectrum is thus imaged onto a (nowadays) CCD camera thanks to a coupling optics. An EELS spectrum, generally consists in the following parts: an intense peak, called "zero-loss peak" (ZLP) because it contains only electrons that have *not* inelastically interacted with the sample in a measurable way, followed by the so-called low loss region (from typically 0.5 to 100 eV), and the core-loss region (from typically 100 eV to several keV). The latter contains valuable information about the chemistry, valence, bonding state and more generally the electronic structure and is now a widespread technique that is able to collect such an information down to the single atomic column [4,5]. In the following, only the IR/VIS/UV part of the spectrum is considered. It is worth noting that this range corresponds to a very restricted part of the huge dynamics in a typical EELS spectrum.

In a CL experiment, a fast electron is sent onto a sample of interest, and the emitted light is collected thanks to a collection optics which can be a curved (paraboloidal or ellipsoidal) or flat mirror, an optical guide, an objective or a lens. The light is then transferred to a spectrometer coupled to a CCD camera and/or a serial detector. The physical content of a CL spectrum is very close to a photoluminescence or scattering spectrum.

### 2.2. Technical bottlenecks

The data presented in this review are almost all dating from the second half of the 2000s or later, although both EELS and CL are more than half a century old techniques. It is thus worth spending some time to explain where the bottlenecks were and what has changed in the past few years. As a general statement, the requirements for reaching at the same time the relevant spatial resolution, spectral resolution, spectral range and relevant signal to noise ratio in both EELS and CL were only very recently reached. Both techniques have immensely benefited from the emergence of high brightness electron guns, allowing to focus the electron beam into very small areas, yet with enough current to generate a decent signal, and from the tremendous development of CCD camera detectors enabling high signal to noise ratio and speed.

In addition, as for EELS, the bottleneck to access the visible range is the presence of the ZLP. This peak has too major drawbacks. First, its Full Width at Half Maximum (FWHM), can be very large (several hundred of meV to several eV), which then limits the spectral resolution of the EELS experiments. Second, its tail can flood the relevant signal in the optical range. The energy profile of the ZLP is related not only to the physical process of emission (thermoionic emission, field effect ...), but also to the high voltage and electron optics instabilities. Different schemes have been developed, including *a posteriori* deconvolution [6] and mains instabilities minimisation [7], and the use of monochromators [8], the later having now popularised the technique and made possible to detect excitations in the hundred of meV range with similar FWHM [9].

As for CL, one limitation has been the lack of systems able to collect at the same time a very high signal and to conserve both the signal and the spectral resolution up to the spectrometer. Such requirements are, indeed, contradictory: even relatively low resolution spectrometers (say, 10 meV) have low numerical apertures (NA). At the same time, in order to conserve the given spectral resolution, the collected light beam diameter has to be small. This is in fact the size of the beam at the entrance of the spectrometer (which can also be reduced at the expense of an intensity loss, through an adjustable slit) which defines the spectral resolution of the spectrometer. The photon beam NA has to match the spectrometer NA in order not to lose intensity within the spectrometer. At the same time, the requirement of collecting a lot of signal implies the use of high NA mirrors (or lenses) after the sample. This means that the actual emission point size (which will be typically diffraction limited) will be highly magnified. The magnification, indeed, scales as the ratio of the NA of the collection optics (which is high) to the one of the spectrometer (which is small). Thus, the image of the emission point onto the entrance of the spectrometer may be larger than the entrance slit of the spectrometer. This results in a drop of signal for a given spectral resolution. It also means that the alignment of the mirror with respect to the specimen has to be extremely precise, and that the field of view can be severely reduced. Indeed, any misalignment from the collection optics with respect to the emission point (and vice versa) is amplified onto the entrance of the spectrometer and may result in the photon beam not hitting the entrance of the spectrometer. Such issues were not present with original systems with either low NA collection optics and/or working in panchromatic mode (see below). However, such systems could not give access to the information dealt with in this review paper. Recent systems [10–12], in Scanning Electron Microscopy (SEM), have at least partly solved these issues thanks to a better design and improvements in mirrors machining, cheap access to aberration corrected lenses, etc. Some of them are now commercially available. The relatively low voltages generally used in SEMs, may have severe drawbacks when addressing nanometer scale optical properties (see Section 4) and as a consequence adaptation of CL systems to STEM is mandatory in many cases.

The situation is however different for STEM-based CL systems, for which commercial equipments exist only sparsely around the world [13,14], but could not give access to the information dealt in this review paper. As a matter of fact, in a STEM, the situation is made even more critical due to the reduced space available within the objective pole-piece. This puts very stringent constraints on the collection optics machining and positioning, a problem which, to the best of our knowledge, has only been solved by our team with the nanoCL system [15].

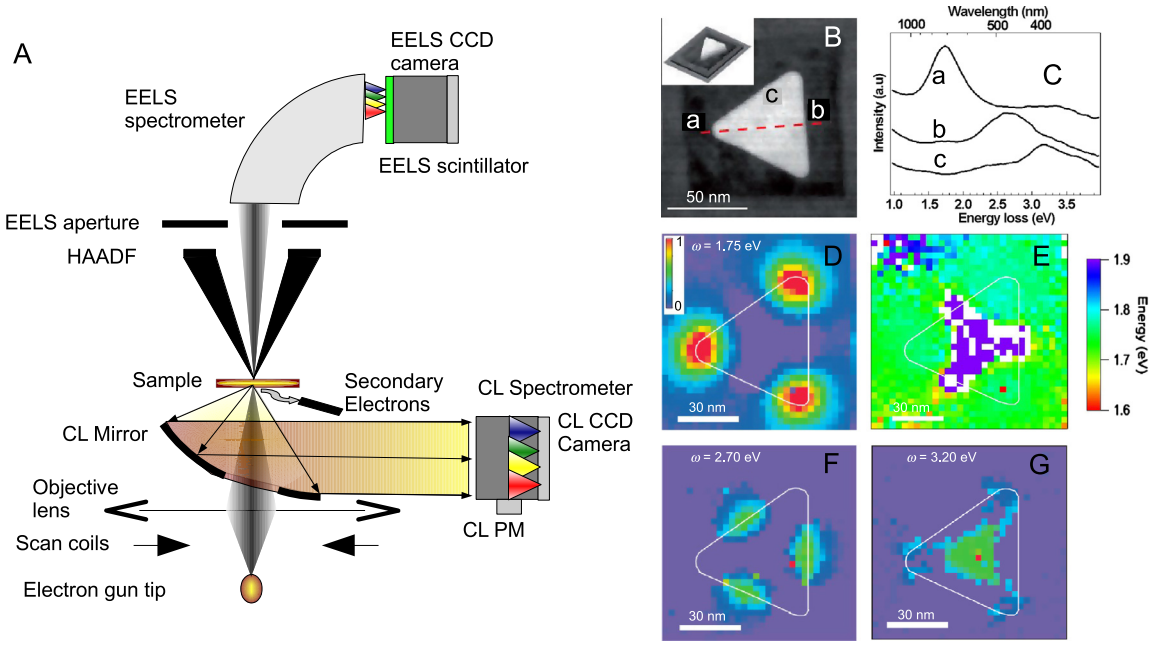


**Fig. 1.** (Colour online.) Principle of spectral imaging with EELS and CL in a STEM. A. Schematic of a STEM fitted with an EELS spectrometer and a CL detection system. B. HAADF image of a flat silver triangle. C. Selection of spectra taken at different positions indicated in B. D. Intensity maps of the lowest energy mode. E. Energy map of the same mode, showing (up to the spectral resolution) a constant energy over the triangle. F. G. Intensity maps of the two next energy modes.

### 2.3. *Spectral imaging*

The spatial resolution, which is at the heart of the interest of the techniques discussed hereafter, is not given only by the fact that the electron beam can be made arbitrary small. In fact, a major interest of EELS and CL experiments for understanding the optics and physics of objects at the nanometer scale relies on the possibility of acquiring *collections* of spectra ("spectral imaging"—SI—[16]), which can be compared with a morphological or structural signal acquired in parallel. This is the spatial variation of the spectral information, and its comparison to the detailed morphology of the object, which really provides access to the richest information.

In practice, an EELS or CL SI experiment works as follows (see Fig. 1). A fast electron beam (from say 1 keV to 40 keV in a SEM, and 40 keV to 300 keV in a STEM) is focused to form an electron probe (typically less than 10 nm in a SEM, less than 1 nm in diameter in a STEM), and scanned over the region of interest. At each position of the probe, several signals can be collected. Signals related to the morphology or the structure (High Angle Annular Dark Field, HAADF, Bright Field, BF, secondary electrons, SE ...) are acquired, so that at the end of the scan an image related to the morphology and/or the structure of the object(s) of interest can be generated. In parallel, either an EELS and/or a CL spectrum is also acquired at each point. At the end of the scan, spectral-images (SI) [17], i.e. images with a spectrum in each pixel, are thus generated. Because both the spectral images and the regular images are acquired in parallel, one can relate each structural information to spectral signatures, pixel per pixel, which is of prime importance for the accuracy of the measurements and the conclusions that can be deduced from the experiments, as shown in the examples selected in this paper. More technical details can be found in Ref. [18].

Other modes of acquisition can be used. For EELS, an alternative method is the Energy Filtered Transmission Electron Microscopy (EFTEM), which, however, has been only sparsely used for nano-optics in the literature [19–21]. In this mode, filtered images are acquired (instead of spectra), and optionally the SI can be generated by stacking energy filtered maps. Interested readers might refer to [22] for a review. For CL, two other modes are also used: in the panchromatic mode, the whole signal can be sent to a serial detector, such as an avalanche diode or a photomultiplier. An image is then acquired with, in each pixel, the signal coming from the serial detector. Alternatively, the CL light can be filtered over some relevant wavelength ranges before hitting the detector, giving rise to filtered images. Although such an acquisition mode was relevant when the parallel detectors were much noisier and slower than the serial detector, it is probably not really the case now, except for special applications (infra-red, single photon detection [23] ...).

Coming back to SI, it is worth noting that *a posteriori* treatments are usually required. Besides the inspection of slices of the full SI, that mimics the filtered images mentioned above, several analysis schemes can be applied to the data. The simplest ones rely on fitting each spectrum with various peak functions. Once the fit is performed, the various quantities extracted from each fit peak can be mapped to generate, e.g energy position maps, amplitude maps, or FWHM maps. This allows to finely map the optical properties of the nano-objects of interest.

Fig. 1 illustrates the different steps for measuring the optical response of metallic nanoparticles with fast electrons, in the specific case of the EELS of a thin silver nanoprism [7]. It is worth noting that such experiments clearly enable to

measure optical properties of a nanoparticle at a deep sub-wavelength scale. This already points to the obvious interest and strength of these electron based techniques over their purely photonic based competitors. However, the nature of the measured quantities, as well as the possibilities and limits of such techniques have to be discussed in detail. The case of plasmons studied by EELS and CL will be developed in the following section, while the case of quantum confined systems, studied by CL, will be tackled in Section 4.

## 3. Plasmons in metallic nanoparticles

### 3.1. Fundamentals

Surface Plasmons (SP) are a mixture of electron density wave and photons which are confined at the interfaces of different materials. Depending on the size of the subtending objects and/or the energy of the plasmons (size and energy are intimately linked, as presented below), SP can be roughly classified into two families. For relatively big objects (larger than the wavelength of light) and low energy, SP behave essentially as (confined) photon modes and are generally referred as Surface Plasmons Polaritons (SPP). They have many potential applications, having both the advantages of photonics (propagation at high speed) and electronics (small dimension features). On the other hand, in small nanoparticles or at relatively larger energy, plasmons are best described as pure electron charge density waves. Such plasmons are sometimes called quasistatic plasmons (as a description in terms of charge density waves, or equivalently in terms of their associated potential, is sufficient to describe them), or localised plasmons. Their interest usually lies in the fact that in small particles they form electromagnetic standing waves, the energy of which can be engineered through tailoring their size and shape. Also, quite importantly, if well designed, they can concentrate the electromagnetic field at a very small scale, making them useful everywhere a field enhancement is necessary.

It is intuitively easy to understand why fast electrons are so good at exciting SP. Indeed, an electron sent in the vicinity or onto an object subtending plasmons will repel the close electrons, which will themselves repel their own neighbouring electrons, and so forth so on, creating a charge density wave which is just the surface plasmons.

This fact was early foreseen by Ritchie [24] for thin films and later revisited by Lucas [25]. Other symmetries like spheres [26], cylinders [27,28] have been theoretically or experimentally tackled in the case of EELS. We note that plasmons have been studied in metals as well as in semiconductors. In the following, we will essentially concentrate on plasmons in gold and silver, as they usually display resonances within or close to the visible range and have thus attracted most of the researchers' attention.

The opposite holds for CL. Indeed, it is not rare in the literature to read that performing CL measurements on metals is pointless. The reasons are probably numerous. The simplest SP, that of a perfect planar interface, does not couple to light and then gives no CL signal. In the case of emitting SP, the Emission (CL) intensity of a plasmonic nanoparticle typically scales as the volume squared, while the absorption (EELS) scales as the volume. Thus, small particles are practically easier to study by EELS, and as large particles may display plasmons energy shifting to the infra-red, studying them by CL can be difficult. Nevertheless, such kind of measurements have been foreseen by J. Garcia de Abajo in 1999 [29]. In 2001, the possibility of performing and understanding CL experiments on silver nanospheres has been demonstrated by Yamamoto et al. [30] in a pioneering paper. To our knowledge, this is the very first paper showing plasmonic eigenmodes mapped with photons generated by fast electrons.

Before making a short survey of the recent theories and simulation tools developed over the past years, a technical point has to be made. Metallic nanostructures are usually either synthesised chemically, or created by lithographic means. EELS experiments, at the opposite to CL ones, require electron-transparent substrates, typically less than few nanometers or tens of nanometers. This is usually not a problem for chemically synthesised nanoparticles which can be simply drop-cast on regular TEM membranes. However, standard techniques, such as electron beam lithography have to be adapted for working with TEM adapted samples [31,32].

### 3.2. Theory

Most of the early theories for describing optical excitations for EELS [24,26,27] or CL [29] of nanoparticles were concerning highly symmetric objects. In these cases, the electromagnetic response of the object is usually characterised by a response function linking the induced field to an exciting field. In the case of a sphere, for example, these are the multipolar polarisabilities, that depend on the angular momentum $l$. The resonances (maxima in the imaginary part of the response functions) appear at the energies of the plasmons. These response functions have analytical forms. In those symmetric cases, the EELS signal can be schematically cast as a sum over all modes (all multipoles in the case of a sphere) of the imaginary part of the response functions, weighted by a position dependent function. This function, as soon as the distance of the electron beam to the surface is larger than few tens of angströms, behaves as a decreasing exponential. In the case of CL, only spheres have been considered analytically [29]. In this case, the result is similar, with the only modification that the imaginary part of the response functions has to be changed to a modulus squared of the very same response functions. We note that the response functions in question are exactly the ones one would measure in optical experiments: for example, in the case of a sphere, we are dealing with multipolar polarisabilities such as they could be defined by opticians [33].

It is however obvious that such a description would fail for experiments such as those presented on Fig. 1, for which the EELS or CL signal is changing very rapidly at the scale of the nanoparticles, and for which polarisabilities are hardly defined. Also, the link to optical quantities and to the electromagnetic eigenmodes of the system is missing.

After the early works on highly symmetric nano-objects, a conceptual step was made by showing that the spatially resolved EELS and CL signals were very close to a quantity called the ElectroMagnetic Local Density Of State (EMLDOS) [7,34]. Such a finding followed similar considerations for comparing the EELS signal in porous alumina to its (non-local) ElectroMagnetic Density of States [35]. The EMLDOS is a very powerful quantity for the characterisation of electromagnetic eigenmodes of a given system. Indeed, it gives, at any given point in space, and at any given energy, the probability of finding a given eigenmode [36]. At the difference to other kind of LDOS (such as the electronic local density of states, which is so convenient to discuss Scanning Tunnelling Microscopy experiments [37]), the EMLDOS is a vectorial quantity. Indeed, the quantities directly related to the EMLDOS are the eigen-electrical fields associated to the eigenmodes, and not the (scalar) eigencharges. As a consequence, EELS is closely related to the mapping of the projection along the electron path of the eigen-electrical fields. Although not exactly equal in the case of nanoparticles, as devised in the initial paper [29] and refined latter on by Hohenester, Ditlbacher and Krenn [38], a clear correspondence can be made between EELS and the eigenmodes of the nanoparticles. This is also true for CL, but to a smaller extent, as non-radiative modes cannot be measured with this technique.

It is useful to present a modal decomposition of the EMLDOS and of the EELS to refine our understanding of both quantities. Unfortunately, such a decomposition was limited to the EMLDOS alone, and specifically to the non-dissipative, purely photonic (i.e. no plasmons) cases [39]. However, very recently, a similar decomposition has been given for both EMLDOS and EELS in the quasistatic regime with an arbitrary dielectric constant (optionally highly dissipative) used for the description of the metal [40]. Although limited to the quasistatic regime, such a decomposition helps at understanding the meaning of the EMLDOS and its relationship to the EELS.

In the restricted but pedagogical case of the Drude model, the EMLDOS at point $\vec{r} = (\vec{R}, z)$ and energy $\omega$, projected along the $z$ direction (zEMLDOS) reads [40]:

$$\rho_z(\vec{r},\omega) = \frac{1}{2\pi^2\omega}\sum_i \Im\left(\frac{\omega_i^2}{\omega^2-\omega_i^2-i\gamma\omega}\right)\left|E_i^z(\vec{r})\right|^2 \tag{1}$$

and the EELS spectrum at point $\vec{r} = (\vec{R}, z)$ (when the electron beam goes along $z$):

$$\Gamma(\vec{r},\omega) = \frac{e^2}{\pi\hbar\omega^2}\sum_i \Im\left(\frac{\omega_i^2}{\omega^2-\omega_i^2-i\gamma\omega}\right)\left|\tilde{E}_i^z(\vec{R},\omega/v)\right|^2 \tag{2}$$

Here, $\omega_i$ is the resonant energy of the mode $i$, $\gamma$ is the dissipation term in the Drude model, $E_i^z(\vec{r})$ is the projection along $z$ of the eigen-electrical field related to mode $i$, and $\tilde{E}_i^z(\vec{R},\omega/v)$ its Fourier transform along $z$.

$\omega_i = \frac{\omega_p}{\sqrt{2}}\sqrt{1+\lambda_i}$ is the plasmon energy of mode $i$ where $\omega_p$ is the bulk plasmon energy, $\{\lambda_i\}$ are a set of real values that only depend on the geometry of the object of interest [41,42]. As an example, $\lambda_i = 0$ for a plane, and $\lambda_i = -1/3$ for the dipolar mode of a sphere, which gives the expected values of the surface plasmons in the Drude model.

When the dissipation is negligible, the imaginary part of the response function for the $i$ mode

$$\Im\left(\frac{\omega_i^2}{\omega^2-\omega_i^2-i\gamma\omega}\right) = \frac{\pi}{2}\omega\delta(\omega-\omega_i)$$

showing that the response function peaks at the surface plasmon resonance frequency.

Eq. (1) has a clear meaning. The EMLDOS varies in space as the square of the eigen electrical field associated to a given mode. In energy, it varies as the response function does (with sharp maxima near the energies of the plasmon eigenmodes). The notion of "local density of states" has an obvious meaning here. As an example, note that when $\lambda_i = -1/3$ ($=0$), the response function reduces to quantities proportional to the dipolar polarisability of a sphere (Fresnel coefficient for a plane). Thus, the response function can be seen as an extension of the notion of polarisability to an arbitrary shape.

Now, the link between EELS and EMLDOS in the special case of the quasistatic limit is obvious from the comparison between Eqs. (2) and (1), showing that, up to a Fourier transform along the electron beam path direction, both quantities are similar. More, the link between EELS and the eigenmodes of the system (through their eigenfield spatial distribution and energies), is made obvious. The EMLDOS is a very widespread concept in nano-optics, and the evidence of a strong link between the EELS (and CL [34]) and the EMLDOS makes the comparison with optical experiments easier.

Independently of the notion of EMLDOS, the link between the EELS, the eigenpotential, the eigenfields and the eigencharge spatial distributions has been discussed in detail in [31,40]. Very recently, this analysis has been drastically improved by Hörl et al. [43]. They have shown theoretically that, in the quasistatic limit, the eigenpotential, and even the eigen-surface charges variations in space (i.e. with no Fourier transform along the electron path) could be retrieved from EELS measurements [43]. This relies on a tomographic reconstruction approach, meaning that a whole sequence of tilted SI have to be acquired to allow further 3D reconstruction of the above-mentioned quantities.

Such a tomographic approach has been experimentally successfully applied on EELS data to silver nanocubes [44]. The interpretation in terms of modes was also based on the modal decomposition of EELS [40,29]. However, the extension to the relativistic regime, where the concepts of eigenpotentials or eigencharges are not sufficient alone to describe the plasmon physics still remains highly challenging.

Different heuristics, simulations or theories have also been developed to reconcile optics with photons and electrons [45,46,21,47] without using the concept of EMLDOS.

Finally, even if the in-depth understanding of EELS and CL has not yet been reached, simulation tools have been developed and shown to be very efficient for modelling EELS and CL data with impressive results. Spectral domain approaches, like the Boundary Element Methods (BEM) [41,42,48,49] and the Discrete Dipole Approximation [50,47], both inheriting from the seminal work of Fuchs [51], and time domain approaches [21,52], have shown interesting results, with some of the codes [50,49,47] being freely available.

### 3.3. Applications

EELS and CL have been used to investigate the physics of plasmons in metallic nanoparticles or nanostructured systems in many different situations.

For the reasons explained above, CL is usually better suited to the study of large and/or thick nanostructures which exhibit a relatively large radiation probability and sustain relativistic, propagating modes. This encompasses many situations with dimensions essentially of the order or larger than the wavelength of light: very thick nanowires [53–55], optionally with angular resolution [56], nanostructured surfaces (for plasmon launching, [57], with rectangular shapes [58]), groves [11], plasmon crystals [59,60], plasmonic Yugi-Uda nanoantennas [61], among others. Few smaller systems like individual nanoparticles have also been investigated, following the milestone work of Yamamoto on silver spheres [30], and latter the work on triangular prisms [52] and decahedra [62,63].

At the opposite, EELS is well adapted to the study of sub-wavelength objects, and numerous works have been reported on individual nanoparticles: spheres or short rods [4,64], triangular systems [19,45,20,21], meta-atoms (curved antennas) [31,65,66], nanoantennas [46,67,9], disks [68], decahedra [62], cubes [69], nanostars [70,71], nano-carrots [72], coupled systems [73,74,32,75–78,66] or more complex geometrical configurations [79–81] and bimetallic systems [82].

As compared to other near-field optical techniques, EELS and CL, especially in the spectral-imaging mode, exhibit specific interests when:

- Spatial and spectral aspects are entangled
- Spatial resolution matters
- Accessing dark modes matters (for EELS)
- Everywhere going outside the visible range matters (for EELS)

In the following, we will illustrate how some of these peculiarities have been exploited to unravel specific plasmon properties.

#### 3.3.1. Nanoresonators

*Definition and physical properties.* Loosely speaking, surface plasmons are a combination of electron density and electromagnetic waves that live at the surface of nanoparticles (metallic in this paper). As the size of the particles decreases to be of the order or less than the typical wavelength of light, boundary conditions are such that the SP are confined. This leads to the appearance of quantized momenta, and thus quantized energies. The nanoparticle acts as a plasmonic cavity or resonator. One directly understands that the plasmon energy, and thus the optical properties, will depend on the size and shape of the resonator. At the intra-particle level, one also understands that each mode (with a given energy) of the resonator will have a different spatial pattern. Both the spatial pattern and the energy can be easily measured in spatially resolved EELS and/or CL experiments. From the relation between energy (measured in the spectrum) and the wavelength of the eigenmodes (measured directly on the maps), one can deduce dispersion relations that are useful to understand the physics of the underlying plasmons. Such dispersion relations can also be unravelled by pure optical means [83–86], but usually on a much narrower energy range, not easily on the same individual nanoparticles, or without direct evidence of the order of the investigated eigenmodes. In the following, we will exemplify the use of dispersion relations to unravel the physics of surface plasmons in nanoresonators.

*Nanorods.* Nanorods are the simplest example of nanoresonators. They are also the simplest examples of plasmonic nanoantennas [87], i.e. plasmonic structures able to convert far field energy to near field one, and vice-versa. Nanorods have a series of eigenmodes of increasing orders, each of them corresponding to an increasing number of charge oscillations of even/odd order. This starts with a dipolar (+|-) mode, followed by a quadrupolar mode (+|–|+) etc. … Such a series is exemplified on the EELS [46] and CL [54] examples of Fig. 2, and have been investigated by a series of authors [55,31,46,67,88]. Note that both EELS and CL are related to the zEMLDOS (the $z$ projected EMLDOS), and thus are more related to the square of the eigencharges [40]. For very small nanoparticles, only the dipolar mode can couple to the far field.

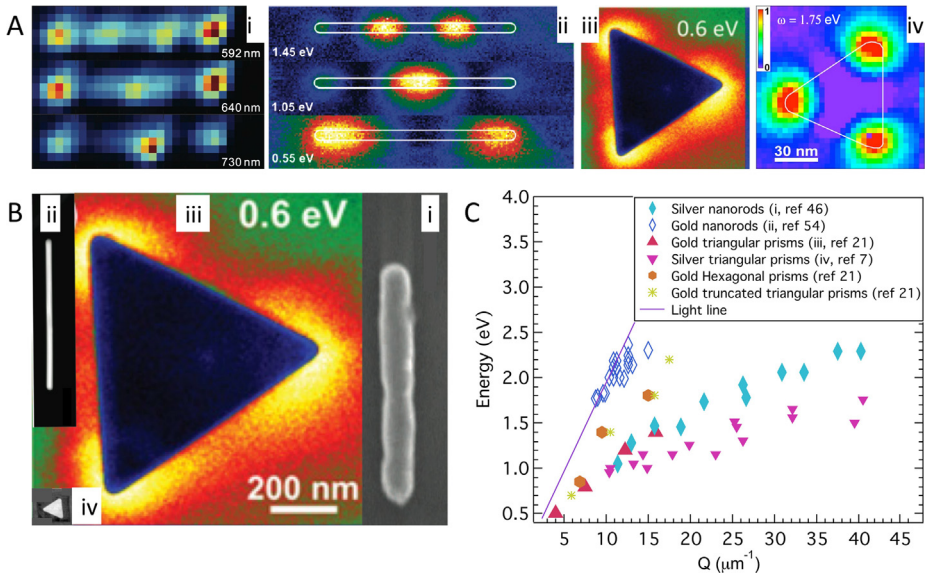


**Fig. 2.** (Colour online.) Plasmon mapping of nanoresonators: size effects and dispersion relations. A. Maps of the first modes for: i. a long and large (short aspect ratio) nanorod (after [54], CL, courtesy A. Polman) and ii. of a shorter one, with a high aspect ratio (after [46] EELS, courtesy D. Rossouw and G. Botton). iii. Maps of the dipolar mode for a long and thick triangular prism [21] (courtesy W. Sigle) and iv. for a small, short aspect ratio one [7]. B. All the former objects are shown on the same scale so that the huge differences in sizes can be clearly visualized. C. Dispersion relations (energy vs. the transferred wavevector $Q$) for different resonators including the four above-mentioned ones.

A quick glance would suggest to the reader that in the two experiments represented on Fig. 2A (i and ii) the plasmons are all the same. This is not true. Indeed, the typical sizes of the rods are quite different (see Fig. 2B); also in both cases, high order multipoles are seen, which is expected for EELS irrespective of the nature of the modes, but indicative of the presence of fundamentally radiative modes for CL. Fig. 2C displays the dispersion relation of both types of nanorods. The differences are obvious, with one following closely the light line, while the other does not. This indicates that the plasmons studied in [89] on large and long nanorods are Surface Plasmon Polaritons, i.e. essentially compressed light modes while the others [46] on high aspect-ratio nanorods are clearly quasistatic plasmons. This discrimination will be further discussed later.

More information can be deduced from the inspection of the dispersion relation. In the case of Split Ring Resonators, which are nanorods bent so that they form a “U” shape (a well-known example of the basic building blocks of metamaterials), the very same series of modes are observed in the EELS plasmons maps [31,88]. This means that to first order, the nanorods modes are not influenced by the bending. However, the analysis of the dispersion relations extracted from EELS spectral imaging allows to identify slight deviations from the ideal straight rods, that reveal the effect of coupling between both arms of the “U” that does not exist in straight rods [31].

*Flat prisms.* Flat prisms are yet another kind of nanoresonators. Such structures are quite important, as they appear naturally during synthesis (most likely in the form of triangles and hexagons), and can be created by electron- or photolithography. A large number of EELS and CL studies have been devoted to such structures [7,19,90,45,21,32,68,52].

As for the nanorods, dispersion relations are helpful to understand the physics of the plasmons. Fig. 2C shows the results for micrometer [91] and nanometer [45] sized triangular nanoprisms. The spatial distributions of the modes are looking pretty much the same, despite the huge difference in the size of the resonators (see Fig. 2B). The dispersion relations, again, are totally different, yet. For the big prisms, it remains close to the light line, and is pretty much the same as for the big rods. In fact, these modes have almost the same behaviour, whatever the geometry of the subtending objects, indicating again a surface polariton nature—a confined wave light propagating along the edge of the structure. For the smaller triangles, the physics is completely different. The dispersion relation, strongly departing from the light line, follows the trend of confined waves in a thin slab, sometimes called Short Range Plasmons [2] (SRP), quasistatic in this case (QSSRP) [45].

Similar dispersion relations arise in circular nanoprisms [68]. In this later case, though, two types of modes emerge (regular ones and radial breathing like modes), with slightly different dispersion relations.

### 3.3.2. Coupling

Electromagnetic coupling between metallic nanoparticles is an important field in plasmonics. When two particles are getting close, plasmons of both particles hybridize leading to a new set of modes. Both the energy position and the spatial distribution of the modes are then changed, allowing a precise engineering of the energy of the modes, of the spatial position of the maxima and their intensity. The main requirement for the coupling to appear is a spatial and spectral overlap between the different modes. A very popular example is that of two or more identical particles close together

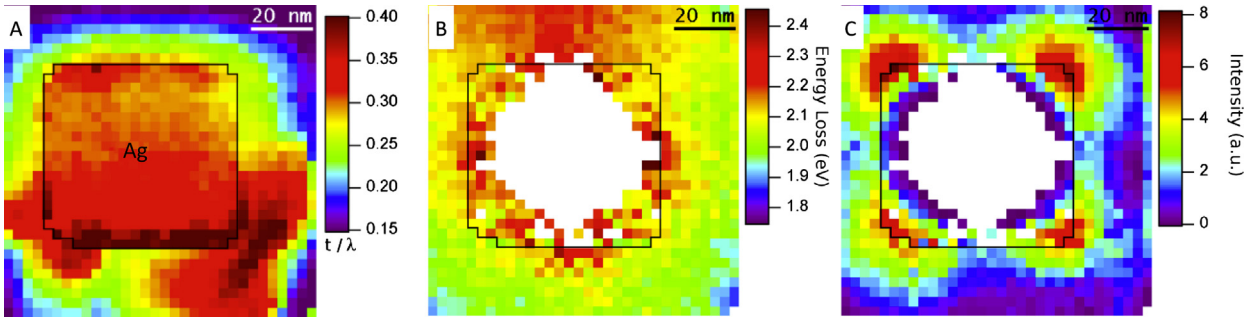


**Fig. 3.** (Colour online.) Example of ultra-local modification of optical properties of a metallic nano-object due to its local environment. A. $t/\lambda$ (thickness in units of the incident electron mean free path) maps of a silver nanocube. One clearly sees the increases in thickness due to the presence of deposited carbon. B. Energy peak position map of the corner mode. At the two bottom corners, a redshift is observed. C. Intensity map of the corner mode. At the two bottom corners, a damping is observed. The boundaries of the Ag cube are outlined with a black line in the three images.

enough so that their dipolar (or higher) modes can couple. One of the reasons of the interest for this situation is due to the fact that in such a coupling, the low energy mode created has a very high intensity within the gap between the particles. This increase in intensity is used for many applications, like Surface Enhanced Raman Scattering [92,93]. This situation has been already studied in the pioneering work of Batson [94], at that time in spot mode, and comprehensively interpreted and simulated by Zabala and coworkers [95]. It is worth noting that one of the interesting, although disappointing result of the work of Zabala and coworkers is that the field within the gap is usually quite difficult to measure. Indeed, the associated electrical field lines are basically perpendicular to electron beam path, therefore producing no loss, and the mode is not detectable within the gap if no tilt is achieved. It is quite ironical to see that the techniques which have the best spatial resolutions are quite blind to an effect that arises at the smallest of the distances.

With the above described capabilities for mapping plasmons, several works have been devoted to the coupling of nanorods [74,75], slits [96] and triangles [32,78]. These studies have essentially confirmed the classical theory of hybridisation, without the need to inject any quantum ingredient in it, although the distances between particles could be smaller than a nanometer. At these distances, non-local effects [97] are expected, and also plasmon assisted electron tunnelling, which has been indirectly seen through a decrease of EELS intensity with respect to the classical theory [76].

### *3.3.3. Ultralocal modification of the plasmons properties in nanoparticles*

Most previous outputs could have been deduced, probably with more difficulties, from pure optical means, or are confirmations of known theories. However, some physical effects, involving highly non-symmetrical shapes, or non-symmetrical coupling, could probably hardly be studied with conventional optical tools, and hardly predicted.

This is the case of the gold nanostars [93,70,71]. Such structures are ca 100 nm in size, with a more or less spherical core and peaked with several tips proturing out. These structures have been studied by standard optical tools (without spatial resolution), giving limited information on their optical properties, due to the complex set of the measured modes, which were highly dependent on the investigated nanostars and on the polarisation of light. However, hope was that the tips would exhibit a field enhancement—favourable for a strong SERS—, which has been proved by EELS later [93]. The modes could be classified as related to the core or the tips [70]. It was shown that each individual tip could have a different plasmon energy. This seems surprising at first sight for a deep sub-wavelength object, which should naively act as a resonator whatever the complexity of its shape (as this has been demonstrated for bent nanoantennas [31,9]). In the case of nanostars, each tip acts as a nanoresonator, decoupled from the other through a core typically larger than the skin depth [70]. Nanostars have also been used as test objects for dealing with the dissipation of plasmons. Despite their tortuous shapes, they have been shown to exhibit plasmons with dissipation rates limited by the intrinsic ohmic loss of the metal, just like standard nanorods [71].

Another example of the interest of using EELS or CL to unravel new effects is the situation where the symmetry of the problem is broken by a change of the nanometer scale environment. Fig. 3 shows EELS maps (energy and intensity) taken on a silver nanocube. Nanocubes are well-known plasmonic nanostructures exhibiting plasmon modes, the intensity of which peaks at the corner (extension to other modes can be found in [51,69]). Such modes can be modified by placing the cubes on a dielectric substrate inducing a symmetry breaking and the emergence of two different modes (one for the corners close to the surface and one for those not in contact to the surface), as demonstrated and analysed in a series of theoretical and experimental studies [98,99] using photonics techniques, and confirmed by EELS [69]. However, the modes in nanocubes appear to be surprisingly even more localised. Indeed, the presence of carboneous material, deposited during experiments at specific corners, influences the energy and intensity at the specific location of the carboneous deposit. This effect occurs on a ten of nanometers, confirming the impressive possibility of monitoring surface plasmons properties at this scale. As for the nanostars, the fact that each corner is affected independently shows that the cube does not act as a resonator as a whole, despite its sub-100 nm length, but each corner does. In this case, the presence of carbon damps and red-shifts the corner plasmon, as expected when a resonator is coupled to a dissipative environment. Similar effects have been observed on gold decahedra by EELS [62] and CL [63].

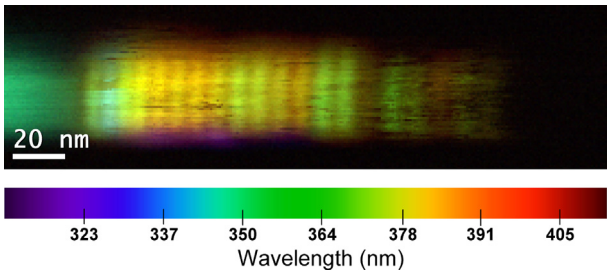


**Fig. 4.** (Colour online.) Multicolour CL image obtained on a stack of GaN Quantum Discs (QDiscs) embedded in an AlN nanowire. This image has been obtained by colouring each wavelength filtered image of a CL SI with the false colour corresponding to the wavelength (see bottom scale), and then overlapping each of them without any other data treatment.

## 4. Luminescence of nanostructured semiconductors

### *4.1. Motivations*

CL is well known for investigating the optical properties of semiconductors. As the size of the structures of interest decreases, dedicated tools have to be developed, especially because the relevant scale for many semiconducting nanostructures or heterostructures is of the order of a nanometer.

Indeed, such materials have demonstrated huge potential interests in a vast amount of technological domains [100] ranging from photodetection [101] to photovoltaics [102] and quantum information [103]. In most cases, the basic properties (luminescence energy) directly depend on the shape and size of the heterostructure, if we are dealing with quantum confined structures, or on the presence of defects and inhomogeneities. As these properties do change at very small scales, one is left with the option of using electron based techniques, at a high spatial resolution, and possibly in conjunction with high resolution imaging. Now, it is worth noting that using CL (as opposite to EELS) has several benefits. This is a luminescence technique, thus one expects to measure peaks and not broad bands, the spectral resolution is at least one order of magnitude better, and some of the nasty effects due to the Coulomb delocalisation [104] do not show up.

There are, however, serious drawbacks that make CL quite challenging, and *a priori* not reliable. Not every system is likely to luminesce, and even if it does, the signal can be extremely weak—which is also the case for plasmons, as noted in Section 3. Also, if one wants to keep a good spectral resolution with a decent signal to noise ratio, a special system has to be designed with challenging constraints when incorporated in a STEM (see Section 1). Furthermore, the spatial resolution can be much worse than the size of the electron probe (see below). However, STEM CL has noticeable advantages and deserves the challenge. Indeed, the CL process in a semiconductor is as follows. The electron beam creates electron–hole pairs (often through the preliminary creation of a plasmon that subsequently decays as electron hole pairs) of various energies. If the sample is thick, the incoming electron suffers a large number of inelastic and elastic collisions and is scattered inside the sample, until all its energy is released. Through phonons emission, the electrons (holes) reach their local minima (maxima) in the energy bands at the point where they have been created. Due to the above mentioned deflections of the incoming electron, the volume in which the electron hole pairs are created can be rather large (up to microns in SEMs). Also, the electrons and the holes can diffuse and drift, leading to yet another source of spatial resolution broadening, as the electrons and holes can then recombine far from the actual excitation point. All these drawbacks have left the idea that CL would be doomed with a very bad spatial resolution [105].

A STEM approach (as compared to a SEM one) has at least two advantages in terms of spatial resolution. The electron beam can be made arbitrary small (well below a nanometer). The high voltage used makes the interaction between the incoming electron and the sample much reduced. Therefore, the broadening ("excitation pear") of the electron probe essentially vanishes in thin samples. Also, the inelastic interaction being much smaller, heating effects and non-linearities, that often affect CL results in semiconductors [106,107], can be expected to be weakened.

### *4.2. III–V heterostructures*

III–V heterostructures are excellent candidates to be investigated by the nanoCL tools, as some of them jointly present small sizes and strong luminescence. As a particular example, let us focus on compounds based on (Ga,In,Al)/(N,As,P), for which various applications already exist [100]. Especially, composite systems incorporating quantum confined structures (quantum wells, quantum dots) are of interest. InAs quantum dots embedded in GaAs [108] or individual quantum dots in cubic GaN [109], core-shell GaN/AlGaN nanowires [14], or stacks of AlGaN quantum wells in AlN nanowires [106] have been studied by CL. Also, GaAs nanostructures have been investigated by spatially and time-resolved CL [10]. Despite the great deal of interest related to the gain in spatial resolution with respect to the photon based spectroscopies, the true size of confinement (say, few nanometers) was not reached. Also, individual structures in densely packed systems (i.e. a few nanometers apart), such as multilayers, had not been addressed.

The probable reason is the lack of combined spatial and spectral resolution, that leads to ambiguities in the assignment of spectral features to a given structure.

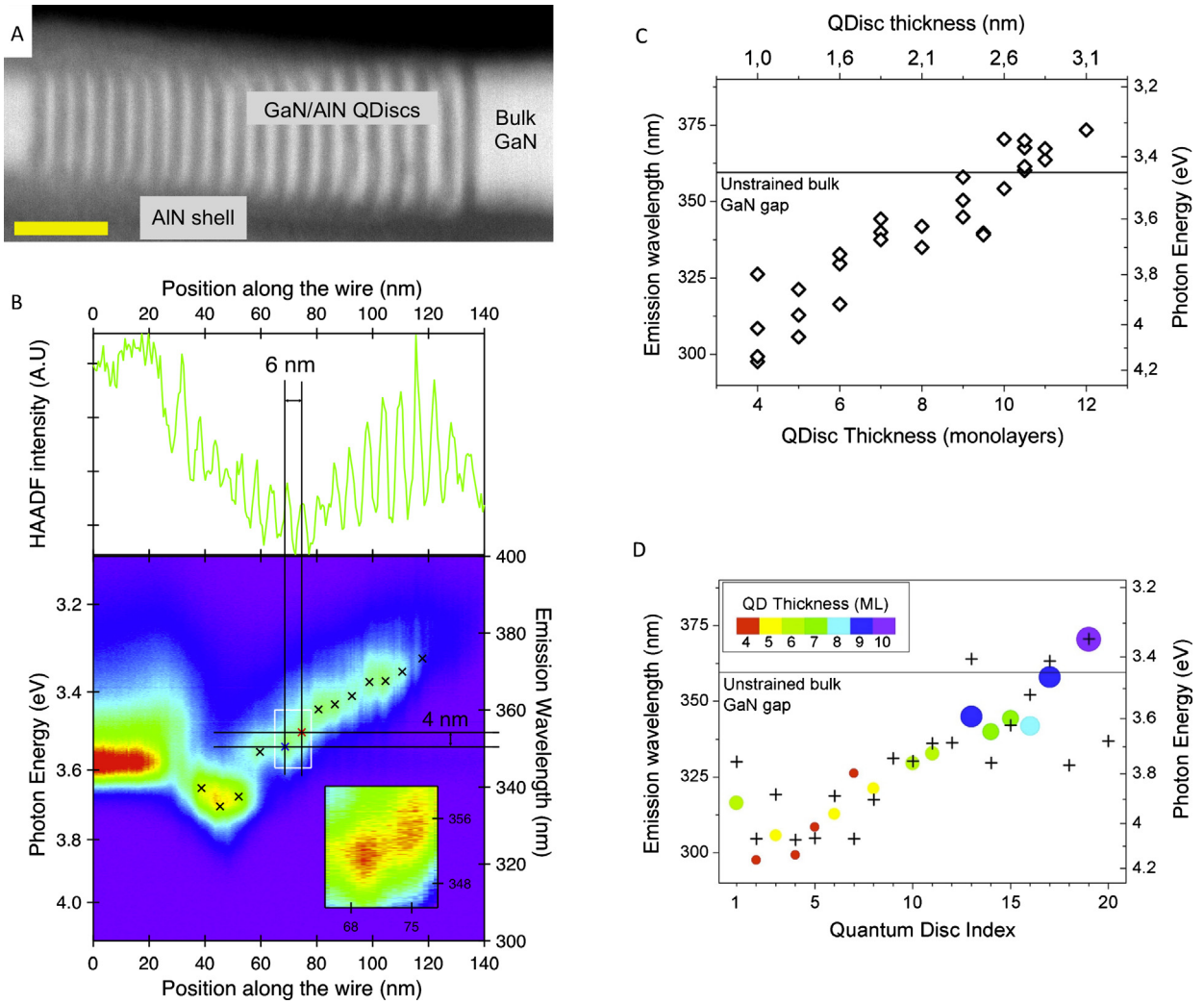


**Fig. 5.** (Colour online.) Spatial and spectral identification of individual Quantum Discs stacked in a nanowire. A. HAADF of a nanowire containing a stack of GaN QDiscs embedded in an AlN shell. GaN appears bright, AlN dark. The growth direction is from left to right. Scale bar is 20 nm. B. 2D plot of a one-dimensional SI. Wavelength versus electron probe location is shown. On top is the HAADF profile acquired during the one-dimensional SI. Inset: magnification of part of the plot showing that individual QDiscs signatures consist in well separated 2D maxima in the wavelength/position space. Note how these maxima correspond to HAADF ones, i.e. to the presence of GaN. C. Dispersion relation for the QDiscs of two nanowires. D. Wavelength versus disc position for an individual nanowire (crosses are simulations). The Qdisc index increases along the growth direction. Note the redshift for a given QDisc thickness as the QDisc shell thickness decreases. After [15].

Also, the link to the atomically resolved structure, which can be mandatory for studying the relationship between emission wavelength and size in quantum confined structure, was missing.

This renders difficult the study of heterostructures embedded in nanowires, such as GaN quantum wells (or quantum discs—QDiscs—in this case) in AlN, for which the QDiscs are only few tens of angströms in thickness and separated by only a few nanometers [110,111] or any other related systems of the (Al,Ga,In)N family [112,113]. For all these reasons, it seemed reasonable to use a STEM based CL system on such relatively thin samples.

Fig. 4 presents a multicolour CL image obtained on a stack of GaN Quantum Discs (QDiscs) embedded in an AlN nanowire. This image has been obtained by colouring each wavelength filtered image of a CL SI with the false colour corresponding to the wavelength, and then overlapping each of them (simply adding the colour of each pixel) without any other data treatment. Such an image strikingly suggests that even on raw data the spatial and spectral resolutions obtained with the nanoCL permits to identify individual quantum objects optical properties even in a very small volume. Of course, the SI analysis allows to go much deeper, and this will be analysed in the following.

Fig. 5 presents CL experiments performed on a series of GaN QDiscs embedded in an AlN NW [15], similar to the one just presented. As a consequence of the growth mechanism, the nanowires start with a GaN base embedded in a large AlN shell, the width of which decreases monotically in the QDiscs region to eventually vanish in the top GaN wire region. Such NW had already been studied by microPL [111], and shown to display a large range of different peaks, changing erratically

from one NW to the other. To address these variations, spatially resolved nanoCL experiments had to be performed [15]. Fig. 5B shows a one-dimensional CL spectral-image (step size 0.6 nm, spectral resolution 0.36 nm) obtained on such a nanowire in the form of a 2D (energy vs position) plot. The plot shows a dispersion of the emission energy as a function of the probe position in the QDiscs region, and the embedded GaN region. The base GaN region shows a constant and bright emission, while the top GaN part shows negligible emission, showing the importance of the shell to avoid surface non-radiative recombinations [114]. In the combined spatial-spectral space, the emission exhibits clearly separated islands (see inset of Fig. 5B), which can be related to individual Quantum Discs emission. This is confirmed by the fact that the centres of the islands peak at the maxima of the inline HAADF profile, i.e. at the QDiscs positions.

It is worth noting that in most cases, adjacent QDiscs display energy differences which are of the order of or even less than the spectral FWHM of the emission peaks. Also, even if the charge carrier delocalisation is weak (1/e decrease is typically 5 nm [114]), the signal of one QDisc overlaps with its first right and left neighbour. For these reasons, filtered images, such as recorded in monochromatic mode, are useless, as the signal filtered at one QDisc energy extends over many different QDiscs. This emphasizes the importance of performing spectral imaging with both high spatial and high spectral resolution, so that identifying the individual QDisc emission properties can be realized unambiguously. We note that this situation resembles that of the measurement of nanorods plasmon dispersion relation (Section 3.3.1), for which spectral imaging is also mandatory. The principle of using spectral imaging to attribute specific luminescence features to a given structure—when filtered imaging or point spectra are failing to do so—has been extended to two-dimensional spectral imaging [114]. In this work intentionally side-grown quantum nanorods could be identified. Note that the use of the full 3D (2 spatial, 1 spectral) information contained in a spectrum-image is common place in EELS [17] and that specific tools such as Principal Component Analysis which may help in extracting this information, have already been used in CL, however in the plasmonic context [115].

This clearly shows that an *ad hoc* use of all the SI information, together with a high efficiency system, is mandatory to retrieve the optical properties of individual Quantum Confined structures in a densely packed architecture. However, it is not sufficient, and such an issue deserves relatively high accelerating voltages which generate smaller excitation volumes. Indeed, despite the use of a state-of-the art CL acquisition system and of extensive SI analysis, the optical properties of individual GaN QDiscs separated by 10 nm could not be disentangled at an accelerating voltage of 5 keV [116].

The comparison of the emission wavelength of each QDisc with its thickness, measured in units of monolayers, allows to understand different physical effects arising in the QDiscs. As seen on Fig. 5C, the dispersion is linear, as expected naively in a particle-in-a-box vision. However, it is worth stressing that such linear dispersion should bend towards the gap energy as the thickness increases, while here, surprisingly, the wavelength (energy) of the QDiscs can be higher (lower) than that of bulk GaN. This is the manifestation of the Quantum Confined Stark Effect [117], i.e. the strong bending of the bands due to an electrical field leading to an increase (decrease) in the emission wavelength (energy) of the quantum confined structure.

Indeed, strong piezo and pyro electrical fields are expected to arise naturally in GaN/AlN structures, and the comparison of the former data to their simulated counterparts allowed to estimate internal electrical field to be of the order of 4 MV/cm, mostly in the form of pyroelectricity. Finally, looking at the energy dispersion of QDiscs of exactly the same thickness within a single NW, it is worth noting a redshift from the base to the top of the wire. This has been attributed to a gradual change of stress along the NW due to a gradual change in shell thickness [15].

### 4.3. Disordered alloys

In the preceding subsection, the objects of interest were quantum confined systems. The spatial resolution was essentially limited by the charge carrier diffusion, as all the other sources of resolution broadening were fixed by using fast electrons for an improved electron probe size and a vanishing excitation pear when working on thin samples (see [114] for a deeper discussion of other effects). The charge carrier diffusion length was itself reduced by the use of III–N systems [118] and the fact that the successive QDiscs act as efficient traps for the charge carriers.

However, in many cases, the needed information concerns defects or structure/compositional local variations. It is therefore surprising to see that valuable information can be extracted from CL measurements, for example on the optical emission at dislocations in diamond [119,120] or at composition changes and fluctuations in (In,Ga)N/GaN epilayers [121]) even if the size of the observed emission was quite large. This specific issue, i.e. the role of the fluctuations of composition in (Al,In,Ga)N alloys, is quite important as it can affect the performance of InGaN photovoltaics devices.

Fig. 6 shows CL spectral imaging on a $Al_xGa_{1-x}N$ nanowire (nominal composition $x = 30$) [122]. A large dispersion of the emission energy can be seen, related to a gradual decrease in the effective Ga content from the tip (right) of the nanowire towards the base (left). This shows how CL can help to map the composition of an alloy [121] at a very reduced scale. More interestingly, localised emission can be identified of typical size around 20 nm which demonstrates that very local alloy fluctuations can also be seen with nanoCL.

### 4.4. Nanometer-scale quantum electrodynamics

Up to this point, we have been dealing with electrons interacting with materials though a classical electromagnetic field. Indeed, in the case of plasmons (Section 3), the plasmons themselves are classically described, their fundamental quantum nature being hidden in the dielectric constant. In the case of semiconducting structures (Section 4), the true quantum

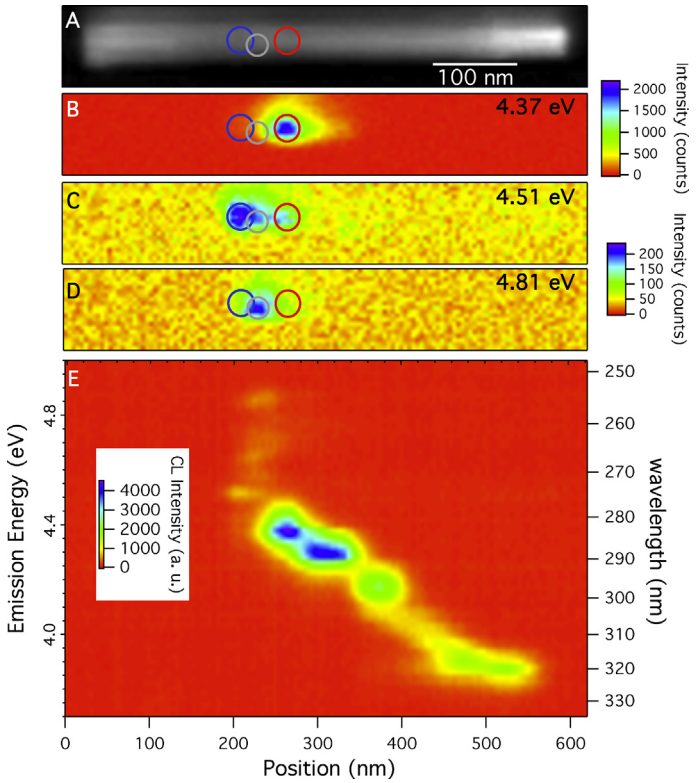


**Fig. 6.** (Colour online.) Localised emission in alloys. A. HAADF of a $Al_xGa_{1-x}N$ nanowire (nominal composition $x = 0.30$). B–C–D: filtered maps extracted from an SI. Very localised features are readily seen. E. 2D plot of the emission energy as a function of the probe position along the nanowire. After [122].

nature of the electrons within the structure is driving all the luminescence results. However, the electromagnetic field keeps being classical. In fact, manifestation of the quantum nature of the electromagnetic field are very sparse—up to a point that W.E. Lamb (the father of the Lamb shift!) in a paper with a provocative title "Anti-Photon" [124] stated that almost all electromagnetic phenomena did not require the concept of photon!

However, one situation requires the introduction of the notion of photon, i.e. the necessity to take into account the corpuscular nature of light. This is the case of Single Photon Emitters (SPE). SPE can be described as two level systems in which only one electron-pair can be present at one moment in an excited state. As such, the light emitted by SPE is made up of only one photon at a time. A more involved description shows that the electromagnetic field states are better described as the so-called "number states" where each mode can be filled by a certain number of photons (1 in the case of single photon emission), and that in such a state the Heisenberg principle reduces to a certainly known number of photons with totally unknown phases (just the opposite to a perfect laser light).

These states cannot be characterised through first order measurements of intensity. They require the measurement of the second order correlation function $g^2(\tau) = \frac{\langle I(t+\tau)I(t)\rangle}{\langle I(t)^2\rangle}$, with $I$, $t$, $\tau$ being the intensity, time and time delay respectively, and $\langle\,\rangle$ is the time average. An SPE would then be revealed by a dip in the correlation function at zero delay, as two photons cannot be detected at the same time. Such effect is called "anti-bunching". This contrasts with the situation of a laser beam, for which the number of photons is totally unknown, and thus the correlation function is flat, and the case of thermal or chaotic light, which may exhibit bunching.

Measurement of the $g^2$ function is usually achieved through an intensity interferometer called an Hanbury Brown and Twiss interferometer (HBT) [125]. As schematised on Fig. 7, an HBT interferometer is simply made up of a beam-splitter that sends the signal to two different high efficiency detectors, the signal of which is time-correlated to give the correlation function.

Single photon states have many practical uses in the quantum information realm [103], and have been actively studied through PL techniques [125]. Simple examples of SPE are Two-Levels Systems (TLS), such as atomic-like structures and real atoms [126], point-like defects [125] or Quantum Dots [127]. Their size is typically comparable to the de Broglie electron wavelength, and as such, order of magnitudes smaller than the typical wavelength of light. Thus, just as for quantum wells (see Section 4.2), one can use PL to study even individual SPE. However, such techniques just fail as soon as two different SPE are separated by less than a light wavelength.

Consequently, the use of CL makes sense to study SPE, in spite of its technical challenge. An SPE has an absolute maximum emission rate given by the lifetime of the emitter. Roughly speaking, the maximum rate is the inverse of the lifetime

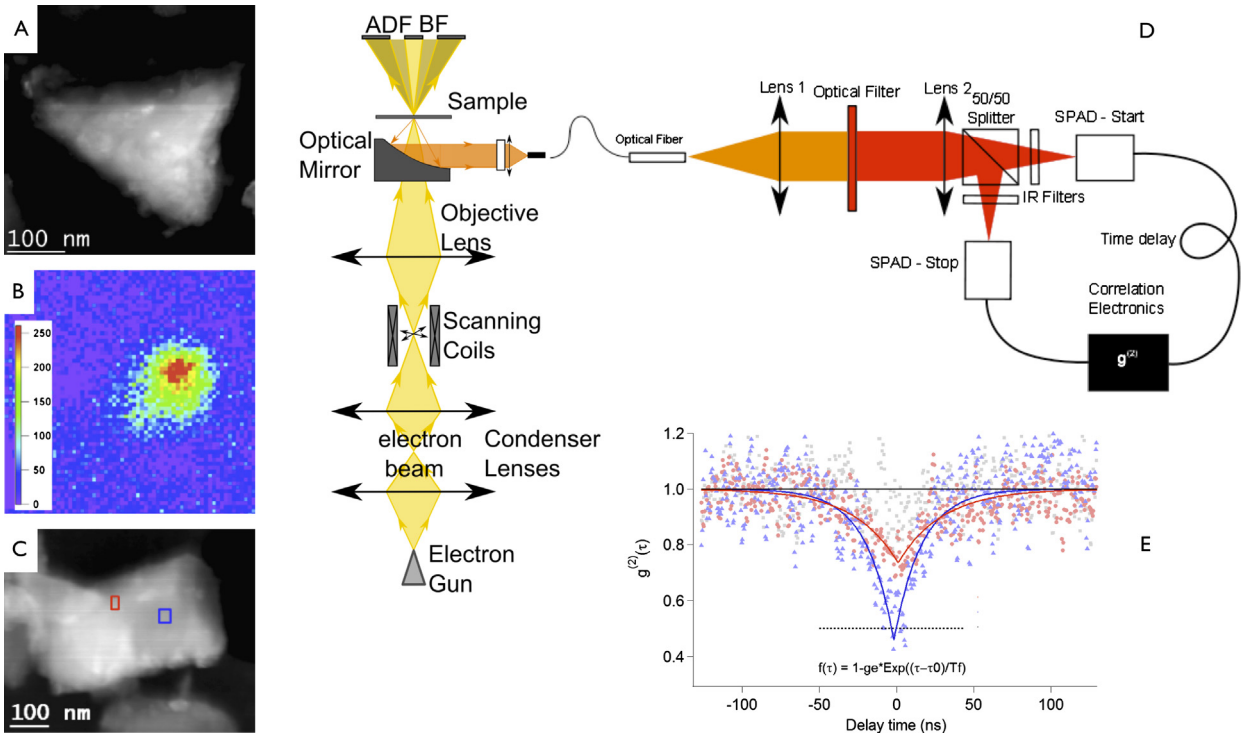


**Fig. 7.** (Colour online.) Quantum electrodynamics in a STEM. A. HAADF of a nanodiamond crystal and B. CL intensity image extracted from a SI around the emission peak of the $NV^0$ centre emission of the same nanodiamond. After [123]. C. HAADF image of another nanodiamond particle. D. Full experimental set up for quantum electrodynamics measurements with fast electrons, including a STEM and an HBT interferometer. E. Correlation functions of the emission of the two coloured areas (red and blue) of C showing a change in the quantum state of the emitted light at sub-wavelength scale. For comparison, the data for classical light emission from another nanoparticle is shown in grey. After [23].

(typically 20 ns in the following example giving a 50 MHz maximum rate) of the emitter, although in practice the rate drops to lower values (hundred of kHz). This rate cannot be increased artificially by increasing the photon (electron) flux in PL (CL). Indeed, a TLS is a highly non-linear system, because upon excitation, no additional states are available. Even worst, too high an excitation can damage the SPE, or induce other types of non-linearities that will depend on the exact electronic structure of the SPE. At the same time, a second order quantity, such as $g^2$, requires much longer acquisition time than a first-order quantity in order to have a sufficient signal-to-noise ratio. Once the optical detection chain is optimised—this has been achieved by the quantum optics community for years—we are left with the need of detecting most of the photons while diminishing as much as possible the electron/sample interaction.

Such a situation requires both an optimised CL system such as the nanoCL system described in [15] and the use of high voltages such as those delivered in a STEM.

Fig. 7D presents the scheme of a STEM coupled to an HBT spectrometer. It has been used to study single photon emission on a very popular type of SPE, the neutral Nitrogen-Vacancy ($NV^0$) centres in nanodiamonds (ND) [125]. These colour centres have a zero-phonon line around 575 nm (emission), and appear naturally in nanodiamonds. $NV^0$ centres (and their charged version, the $NV^-$) are popular candidates for quantum cryptography. They need be integrated into practical devices on sub-wavelength scales. It is thus of importance to measure the quantum state of the emitted light at the nanometer scale. Also, CL has demonstrated to be a very popular and efficient technique for studying diamond and in particular NV centres [128,12]. However, it is very important to understand that the measurement of the intensity alone is not sufficient to prove that a single NV centre has been identified. Indeed, even with a high spatial resolution (see Fig. 7B), the detection of individual defects is ambiguous and needs to rely on single photon detection through an HBT measurement.

Fig. 7E shows the correlation function measured on two different NDs [23]. While the first one displays a flat correlation function, typical of a classical light state, the second exhibits a dip smaller than 0.5, typical of single photon emission. Although this is the first demonstration of a quantum state of light generation through high speed electrons—not to be confused with Electroluminescence [129,130]—, it does not add much to the field of nano-optics with respect to PL. Fig. 7E shows a second anti-bunched curve taken 130 nm apart from the first one. The shape of the curve is changing, proving that different states of light can be generated from the same ND crystal but at positions sub wavelength apart.

The field of quantum electrodynamics with fast electrons is in its infancy, and much has to be understood on the physics of the electron/particle/electromagnetic field interactions. However, the above demonstrated sub-wavelength capabilities are already very promising for the study of quantum information devices.

## 5. Conclusions

In this paper, we have reviewed some recent studies using fast electron based spectroscopies applied to plasmonic nanoparticles and semiconducting nanostructures. The increase in spatial resolution as well as the possibility to compare nanometer per nanometer the optical properties with the structure of the object has shown to be invaluable in various situations. In many cases, EELS acts really as a nanometer counterpart of absorption spectroscopies, while CL acts as a nanometer counterpart of luminescence/scattering spectroscopies. For example, the link between CL and PL is so strong that quantum optical experiments mimicking PL with CL, but with a vast increase of resolution, can be done.

New horizons are however to be explored. In particular, time-resolution together with a nanometer resolution is still to be performed routinely following the impressive first steps in this direction [10]. Together with the use of an external excitation (electrical field, laser injection), it would pave the way to nanometer scale non-linear nano-optics.

## Acknowledgements

We want to thank all the collaborators that have helped us to explore and improve our understanding of the field over the past few years: A. Douiri, J. Nelayah, S. Mazzucco, G. Boudarham, L. Henrard, J. Garcia de Abajo, L. Liz-Marzan, M. Wegener, V. Myroshnychenko, N. Geuquet, M. Tchernycheva, L. Rigutti, F. Julien, G. Jacopin, B. Daudin, A. Pierret, F. Treussart. M.K. wants to thanks J. Barjon for valuable discussions concerning SEM-CL. This work has received support from the National Agency for Research under the program of future investment TEMPOS–CHROMATEM with the Reference No. ANR-10-EQPX-50. The research leading to these results has received funding from the European Union Seventh Framework Programme [No. FP7/2007–2013] under Grant Agreement No. n312483 (ESTEEM2).

## References

[1] E. Rittweger, K.Y. Han, S.E. Irvine, C. Eggeling, S.W. Hell, Sted microscopy reveals crystal colour centres with nanometric resolution, Nat. Photonics 3 (3) (March 2009) 144–147.
[2] L. Douillard, F. Charra, Z. Korczak, R. Bachelot, S. Kostcheev, G. Lerondel, P.M. Adam, P. Royer, Short range plasmon resonators probed by photoemission electron microscopy, Nano Lett. 8 (3) (March 2008) 935–940.
[3] F.J.G. de Abajo, Optical excitations in electron microscopy, Rev. Modern Phys. 82 (2010) 209–275.
[4] M. Bosman, V.J. Keast, J.L. Garcia-Munoz, A.J. D'alfonso, S.D. Findlay, L.J. Allen, Two-dimensional mapping of chemical information at atomic resolution, Phys. Rev. Lett. 99 (8) (August 2007) 086102.
[5] Almudena Torres-Pardo, Alexandre Gloter, Pavlo Zubko, Noémie Jecklin, Céline Lichtensteiger, Christian Colliex, Jean-Marc Triscone, Odile Stéphan, Spectroscopic mapping of local structural distortions in ferroelectric $PbTiO_3/SrTiO_3$ superlattices at the unit-cell scale, Phys. Rev. B 84 (Dec 2011) 220102.
[6] A. Gloter, A. Douiri, M. Tence, C. Colliex, Improving energy resolution of EELS spectra: an alternative to the monochromator solution, Ultramicroscopy 96 (3–4) (2003) 385–400.
[7] J. Nelayah, M. Kociak, O. Stéphan, F.J.G. de Abajo, M. Tencé, L. Henrard, D. Taverna, I. Pastoriza-Santos, L.M. Liz-Marzán, C. Colliex, Mapping surface plasmons on a single metallic nanoparticle, Nat. Phys. 3 (5) (May 2007) 348–353.
[8] M. N'Gom, J. Ringnalda, J.F. Mansfield, A. Agarwal, N. Kotov, N.J. Zaluzec, T.B. Norris, Single particle plasmon spectroscopy of silver nanowires and gold nanorods, Nano Lett. 8 (10) (October 2008) 3200–3204.
[9] D. Rossouw, G.A. Botton, Plasmonic response of bent silver nanowires for nanophotonic subwavelength waveguiding, Phys. Rev. Lett. 110 (6) (February 2013) 066801.
[10] M. Merano, S. Sonderegger, A. Crottini, S. Collin, P. Renucci, E. Pelucchi, A. Malko, M.H. Baier, E. Kapon, B. Deveaud, J.D. Ganiere, Probing carrier dynamics in nanostructures by picosecond cathodoluminescence, Nature 438 (7067) (November 2005) 479–482.
[11] E.J.R. Vesseur, F.J.G. de Abajo, A. Polman, Modal decomposition of surface-plasmon whispering gallery resonators, Nano Lett. 9 (9) (September 2009) 3147–3150.
[12] B. Willems, A. Tallaire, J. Barjon, Exploring the origin and nature of luminescent regions in CVD synthetic diamond, Gems Gemol. 47 (3) (2011) 202–207.
[13] H.P. Strunk, M. Albrecht, H. Scheel, Cathodoluminescence in transmission electron microscopy, J. Microsc. 224 (October 2006) 79–85.
[14] S.K. Lim, M. Brewster, F. Qian, Y. Li, C.M. Lieber, S. Gradecak, Direct correlation between structural and optical properties of III–V nitride nanowire heterostructures with nanoscale resolution, Nano Lett. 9 (11) (November 2009) 3940–3944.
[15] L.F. Zagonel, S. Mazzucco, M. Tence, K. March, R. Bernard, B. Laslier, G. Jacopin, M. Tchernycheva, L. Rigutti, F.H. Julien, R. Songmuang, M. Kociak, Nanometer scale spectral imaging of quantum emitters in nanowires and its correlation to their atomically resolved structure, Nano Lett. 11 (2) (February 2011) 568–573.
[16] C. Jeanguillaume, C. Colliex, Spectrum-image: The next step in EELS digital acquisition and processing, Ultramicroscopy 28 (1–4) (April 1989) 252–257.
[17] C. Colliex, M. Tencé, E. Lefèvre, C. Mory, H. Gu, D. Bouchetand, C. Jeanguillaume, Electron-energy-loss spectroscopy mapping, Mikrochim. Acta 71 (1994) 114–115.
[18] M. Kociak, O. Stéphan Walls M, C. Colliex, Spatially Resolved EELS: The Spectrum-Imaging Technique and Its Applications, Springer, 2011, p. 163, Chapter 4.
[19] J. Nelayah, J. Gu, W. Sigle, C.T. Koch, I. Pastoriza-Santos, L.M. Liz-Marzan, P.A. van Aken, Direct imaging of surface plasmon resonances on single triangular silver nanoprisms at optical wavelength using low-loss eftem imaging, Opt. Lett. 34 (7) (April 2009) 1003–1005.
[20] B. Schaffer, W. Grogger, G. Kothleitner, F. Hofer, Comparison of eftem and stem eels plasmon imaging of gold nanoparticles in a monochromated tem, Ultramicroscopy 110 (8) (July 2010) 1087–1093.
[21] L. Gu, W. Sigle, C.T. Koch, B. Ogut, P.A. van Aken, N. Talebi, R. Vogelgesang, J.L. Mu, X.G. Wen, J. Mao, Resonant wedge-plasmon modes in single-crystalline gold nanoplatelets, Phys. Rev. B 83 (19) (May 2011) 195433.
[22] B. Schaffer, G. Kothleitner, W. Grogger, Eftem spectrum imaging at high-energy resolution, Ultramicroscopy 106 (11–12) (October 2006) 1129–1138.
[23] L.H.G. Tizei, M. Kociak, Spatially resolved quantum nano-optics of single photons using an electron microscope, Phys. Rev. Lett. 110 (15) (April 2013) 153604.
[24] R.H. Ritchie, Plasma losses by fast electrons in thin films, Phys. Rev. 106 (Jun 1957) 874–881.

[25] A.A. Lucas, E. Kartheuser, Energy-loss spectrum of fast electrons in a dielectric slab. I. Nonretarded losses and Cherenkov bulk loss, Phys. Rev. B 1 (May 1970) 3588–3598.
[26] T.L. Ferrell, P.M. Echenique, Generation of surface excitations on dielectric spheres by an external electron beam, Phys. Rev. Lett. 55 (1985) 1526–1529.
[27] N. Zabala, A. Rivacoba, P.M. Echenique, Energy loss of electrons travelling through cylindrical holes, Surf. Sci. 209 (1989) 465–480.
[28] D. Taverna, M. Kociak, V. Charbois, L. Henrard, Electron energy-loss spectrum of an electron passing near a locally anisotropic nanotube, Phys. Rev. B 66 (23) (December 2002) 235419.
[29] F.J. Garcia de Abajo, Relativistic energy loss induced photon emission in the interaction of a dielectric sphere with an external electron beam, Phys. Rev. B 59 (1999) 3095–3107.
[30] N. Yamamoto, K. Araya, F.J.G. de Abajo, Photon emission from silver particles induced by a high-energy electron beam, Phys. Rev. B 6420 (20) (November 2001) 205419.
[31] G. Boudarham, N. Feth, V. Myroshnychenko, S. Linden, F.J.G. de Abajo, M. Wegener, M. Kociak, Spectral imaging of individual split-ring resonators, Phys. Rev. Lett. 105 (25) (Dec 2010) 255501.
[32] A.L. Koh, A.I. Fernandez-Dominguez, D.W. McComb, S.A. Maier, J.K.W. Yang, High-resolution mapping of electron-beam-excited plasmon modes in lithographically defined gold nanostructures, Nano Lett. 11 (3) (March 2011) 1323–1330.
[33] Craig F. Bohren, Donald R. Huffman, Absorption and Scattering of Light by Small Particles, Wiley-VCH Verlag GmbH, 2007.
[34] F.J.G. de Abajo, M. Kociak, Probing the photonic local density of states with electron energy loss spectroscopy, Phys. Rev. Lett. 100 (10) (March 2008) 106804.
[35] F.J.G. de Abajo, A.G. Pattantyus-Abraham, N. Zabala, A. Rivacoba, M.O. Wolf, P.M. Echenique, Cherenkov effect as a probe of photonic nanostructures, Phys. Rev. Lett. 91 (14) (October 2003) 143902.
[36] K. Joulain, R. Carminati, J.P. Mulet, J.J. Greffet, Definition and measurement of the local density of electromagnetic states close to an interface, Phys. Rev. B 68 (24) (December 2003) 245405.
[37] S.G. Lemay, J.W. Janssen, M. van den Hout, M. Mooij, M.J. Bronikowski, P.A. Willis, R.E. Smalley, L.P. Kouwenhoven, C. Dekker, Two-dimensional imaging of electronic wavefunctions in carbon nanotubes, Nature 412 (6847) (August 2001) 617–620.
[38] U. Hohenester, H. Ditlbacher, J.R. Krenn, Electron-energy-loss spectra of plasmonic nanoparticles, Phys. Rev. Lett. 103 (10) (September 2009) 106801.
[39] A. Dereux, C. Girard, J.C. Weeber, Theoretical principles of near-field optical microscopies and spectroscopies, J. Chem. Phys. 112 (18) (May 2000) 7775–7789.
[40] G. Boudarham, M. Kociak, Modal decompositions of the local electromagnetic density of states and spatially resolved electron energy loss probability in terms of geometric modes, Phys. Rev. B 85 (Jun 2012) 245447.
[41] F. Ouyang, M. Isaacson, Accurate modeling of particle substrate coupling of surface-plasmon excitation in eels, Ultramicroscopy 31 (4) (December 1989) 345–350.
[42] F.J. García de Abajo, J. Aizpurua, Numerical simulation of electron energy loss near inhomogeneous dielectrics, Phys. Rev. B 56 (24) (Dec 1997) 15873–15884.
[43] A. Hörl, A. Trügler, U. Hohenester, Tomography of particle plasmon fields from electron energy loss spectroscopy, Phys. Rev. Lett. 111 (Aug 2013) 076801.
[44] O. Nicoletti, F. de la Pena, R.K. Leary, D.J. Holland, C. Ducati, P.A. Midgley, Three-dimensional imaging of localized surface plasmon resonances of metal nanoparticles, Nature 502 (7469) (October 2013) 80–84.
[45] J. Nelayah, M. Kociak, O. Stephan, N. Geuquet, L. Henrard, F.J.G. de Abajo, I. Pastoriza-Santos, L.M. Liz-Marzan, C. Colliex, Two-dimensional quasistatic stationary short range surface plasmons in flat nanoprisms, Nano Lett. 10 (3) (March 2010) 902–907.
[46] D. Rossouw, M. Couillard, J. Vickery, E. Kumacheva, G.A. Botton, Multipolar plasmonic resonances in silver nanowire antennas imaged with a sub-nanometer electron probe, Nano Lett. 11 (4) (April 2011) 1499–1504.
[47] V. Iberi, N. Mirsaleh-Kohan, J.P. Camden, Understanding plasmonic properties in metallic nanostructures by correlating photonic and electronic excitations, J. Phys. Chem. Lett. 4 (7) (April 2013) 1070–1078.
[48] F.J.G. de Abajo, A. Howie, Retarded field calculation of electron energy loss in inhomogeneous dielectrics, Phys. Rev. B 65 (11) (March 2002) 115418.
[49] U. Hohenester, A. Trugler, MNPBEM – a matlab toolbox for the simulation of plasmonic nanoparticles, Comput. Phys. Commun. 183 (2) (February 2012) 370–381.
[50] N. Geuquet, L. Henrard, EELS and optical response of a noble metal nanoparticle in the frame of a discrete dipole approximation, Ultramicroscopy 110 (8) (July 2010) 1075–1080.
[51] R. Fuchs, Theory of the optical properties of ionic crystal cubes, Phys. Rev. B 11 (Feb 1975) 1732–1740.
[52] P. Das, T.K. Chini, J. Pond, Probing higher order surface plasmon modes on individual truncated tetrahedral gold nanoparticle using cathodoluminescence imaging and spectroscopy combined with fdtd simulations, J. Phys. Chem. C 116 (29) (July 2012) 15610–15619.
[53] N. Yamamoto, M. Nakano, T. Suzuki, Light emission by surface plasmons on nanostructures of metal surfaces induced by high-energy electron beams, Surf. Interface Anal. 38 (12–13) (December 2006) 1725–1730.
[54] E.J.R. Vesseur, R. de Waele, M. Kuttge, A. Polman, Direct observation of plasmonic modes in au nanowires using high-resolution cathodoluminescence spectroscopy, Nano Lett. 7 (9) (September 2007) 2843–2846.
[55] R. Gomez-Medina, N. Yamamoto, M. Nakano, F.J.G. Abajo, Mapping plasmons in nanoantennas via cathodoluminescence, New J. Phys. 10 (October 2008) 105009.
[56] T. Coenen, E.J.R. Vesseur, A. Polman, Deep subwavelength spatial characterization of angular emission from single-crystal au plasmonic ridge nanoantennas, ACS Nano 6 (2) (February 2012) 1742–1750.
[57] M.V. Bashevoy, F. Jonsson, K.F. MacDonald, Y. Chen, N.I. Zheludev, Hyperspectral imaging of plasmonic nanostructures with nanoscale resolution, Opt. Express 15 (18) (September 2007) 11313–11320.
[58] M. Kuttge, E.J.R. Vesseur, A. Polman, Fabry–Perot resonators for surface plasmon polaritons probed by cathodoluminescence, Appl. Phys. Lett. 94 (18) (May 2009) 183104.
[59] T. Suzuki, N. Yamamoto, Cathodoluminescent spectroscopic imaging of surface plasmon polaritons in a 1-dimensional plasmonic crystal, Opt. Express 17 (26) (December 2009) 23664–23671.
[60] K. Takeuchi, N. Yamamoto, Visualization of surface plasmon polariton waves in two-dimensional plasmonic crystal by cathodoluminescence, Opt. Express 19 (13) (June 2011) 12365–12374.
[61] T. Coenen, E.J.R. Vesseur, A. Polman, A.F. Koenderink, Directional emission from plasmonic yagi-uda antennas probed by angle-resolved cathodoluminescence spectroscopy, Nano Lett. 11 (9) (September 2011) 3779–3784.
[62] V. Myroshnychenko, J. Nelayah, G. Adamo, N. Geuquet, J. Rodriguez-Fernandez, I. Pastoriza-Santos, K.F. MacDonald, L. Henrard, L.M. Liz-Marzan, N.I. Zheludev, M. Kociak, F.J.G. de Abajo, Plasmon spectroscopy and imaging of individual gold nanodecahedra: A combined optical microscopy, cathodoluminescence, and electron energy-loss spectroscopy study, Nano Lett. 12 (8) (August 2012) 4172–4180.
[63] P. Das, T.K. Chini, Spectroscopy and imaging of plasmonic modes over a single decahedron gold nanoparticle: A combined experimental and numerical study, J. Phys. Chem. C 116 (49) (December 2012) 25969–25976.
[64] M. N'Gom, S.Z. Li, G. Schatz, R. Erni, A. Agarwal, N. Kotov, T.B. Norris, Electron-beam mapping of plasmon resonances in electromagnetically interacting gold nanorods, Phys. Rev. B 80 (11) (September 2009) 113411.

[65] F. von Cube, S. Irsen, S. Linden, From isolated metaatoms to photonic metamaterials: Mapping of collective near-field phenomena with eels, in: 2012 Conference on Lasers and Electro-Optics (CLEO), 2012.
[66] F. von Cube, S. Irsen, R. Diehl, J. Niegemann, K. Busch, S. Linden, From isolated metaatoms to photonic metamaterials: Evolution of the plasmonic near-field, Nano Lett. 13 (2) (February 2013) 703–708.
[67] O. Nicoletti, M. Wubs, N.A. Mortensen, W. Sigle, P.A. van Aken, P.A. Midgley, Surface plasmon modes of a single silver nanorod: an electron energy loss study, Opt. Express 19 (16) (August 2011) 15371–15379.
[68] F.P. Schmidt, H. Ditlbacher, U. Hohenester, A. Hohenau, F. Hofer, J.R. Krenn, Dark plasmonic breathing modes in silver nanodisks, Nano Lett. 12 (11) (November 2012) 5780–5783.
[69] S. Mazzucco, N. Geuquet, J. Ye, O. Stephan, W. Van Roy, P. Van Dorpe, L. Henrard, M. Kociak, Ultralocal modification of surface plasmons properties in silver nanocubes, Nano Lett. 12 (3) (Mar 2012) 1288–1294.
[70] S. Mazzucco, O. Stephan, C. Colliex, I. Pastoriza-Santos, L.M. Liz-Marzan, J.G. de Abajo, M. Kociak, Spatially resolved measurements of plasmonic eigenstates in complex-shaped, asymmetric nanoparticles: gold nanostars, Eur. Phys. J. Appl. Phys. 54 (3) (June 2011) 33512.
[71] M. Bosman, E. Ye, S.F. Tan, C.A. Nijhuis, J.K.W. Yang, R. Marty, A. Mlayah, A. Arbouet, C. Girard, M.Y. Han, Surface plasmon damping quantified with an electron nanoprobe, Sci. Rep. 3 (February 2013) 1312.
[72] Hongyan Liang, David Rossouw, Haiguang Zhao, Scott K. Cushing, Honglong Shi, Andreas Korinek, Hongxing Xu, Federico Rosei, Wenzhong Wang, Nianqiang Wu, Gianluigi A. Botton, Dongling Ma, Asymmetric silver nanocarrot structures: Solution synthesis and their asymmetric plasmonic resonances, J. Am. Chem. Soc. 135 (26) (2013) 9616–9619.
[73] M. Bosman, V.J. Keast, M. Watanabe, A.I. Maaroof, M.B. Cortie, Mapping surface plasmons at the nanometre scale with an electron beam, Nanotechnology 18 (16) (April 2007) 165505.
[74] M.-W. Chu, V. Myroshnychenko, C.-H. Chen, J.-P. Deng, C.-Y. Mou, F.J.G. de Abajo, Probing bright and dark surface-plasmon modes in individual and coupled noble metal nanoparticles using an electron beam, Nano Lett. 9 (1) (2009) 399–404.
[75] I. Alber, W. Sigle, S. Muller, R. Neumann, O. Picht, M. Rauber, P.A. van Aken, M.E. Toimil-Molares, Visualization of multipolar longitudinal and transversal surface plasmon modes in nanowire dimers, ACS Nano 5 (12) (December 2011) 9845–9853.
[76] J.A. Scholl, A. Garcia-Etxarri, A.L. Koh, J.A. Dionne, Observation of quantum tunneling between two plasmonic nanoparticles, Nano Lett. 13 (2) (February 2013) 564–569.
[77] N. Talebi, W. Sigle, R. Vogelgesang, C.T. Koch, C. Fernandez-Lopez, L.M. Liz-Marzan, B. Ogut, M. Rohm, P.A. van Aken, Breaking the mode degeneracy of surface plasmon resonances in a triangular system, Langmuir 28 (24) (June 2012) 8867–8873.
[78] H.G. Duan, A.I. Fernandez-Dominguez, M. Bosman, S.A. Maier, J.K.W. Yang, Nanoplasmonics: Classical down to the nanometer scale, Nano Lett. 12 (3) (March 2012) 1683–1689.
[79] B. Ogut, N. Talebi, R. Vogelgesang, W. Sigle, P.A. van Aken, Toroidal plasmonic eigenmodes in oligomer nanocavities for the visible, Nano Lett. 12 (10) (October 2012) 5239–5244.
[80] M. Bosman, G.R. Anstis, V.J. Keast, J.D. Clarke, M.B. Cortie, Light splitting in nanoporous gold and silver, ACS Nano 6 (1) (January 2012) 319–326.
[81] A. Losquin, S. Camelio, D. Rossouw, M. Besbes, F. Pailloux, D. Babonneau, G.A. Botton, J.-J. Greffet, O. Stéphan, M. Kociak, Experimental evidence of nanometer-scale confinement of plasmonic eigenmodes responsible for hot spots in random metallic films, Phys. Rev. B 88 (Sep 2013) 115427.
[82] B. Rodriguez-Gonzalez, F. Attouchi, M.F. Cardinal, V. Myroshnychenko, O. Stephan, F.J.G. de Abajo, L.M. Liz-Marzan, M. Kociak, Surface plasmon mapping of dumbbell-shaped gold nanorods: The effect of silver coating, Langmuir 28 (24) (June 2012) 9063–9070.
[83] H. Ditlbacher, A. Hohenau, D. Wagner, U. Kreibig, M. Rogers, F. Hofer, F.R. Aussenegg, J.R. Krenn, Silver nanowires as surface plasmon resonators, Phys. Rev. Lett. 95 (25) (December 2005) 257403.
[84] J. Dorfmüller, R. Vogelgesang, R.T. Weitz, C. Rockstuhl, C. Etrich, T. Pertsch, F. Lederer, K. Kern, Fabry–Perot resonances in one-dimensional plasmonic nanostructures, Nano Lett. 9 (6) (2009) 2372–2377.
[85] R. Esteban, R. Vogelgesang, J. Dorfmuller, A. Dmitriev, C. Rockstuhl, C. Etrich, K. Kern, Direct near-field optical imaging of higher order plasmonic resonances, Nano Lett. 8 (10) (October 2008) 3155–3159.
[86] Kohei Imura, Hiromi Okamoto, Development of novel near-field microspectroscopy and imaging of local excitations and wave functions of nanomaterials, Bull. Chem. Soc. Jpn. 81 (2008) 659–675.
[87] L. Novotny, N. van Hulst, Antennas for light, Nat. Photonics 5 (2) (February 2011) 83–90.
[88] F. von Cube, S. Irsen, J. Niegemann, C. Matyssek, W. Hergert, K. Busch, S. Linden, Spatio-spectral characterization of photonic meta-atoms with electron energy-loss spectroscopy [invited], Opt. Mater. Express 1 (5) (September 2011) 1009–1018.
[89] E.J.R. Vesseur, A. Polman, Controlled spontaneous emission in plasmonic whispering gallery antennas, Appl. Phys. Lett. 99 (23) (December 2011) 231112.
[90] P. Chaturvedi, K.H. Hsu, A. Kumar, K.H. Fung, J.C. Mabon, N.X. Fang, Imaging of plasmonic modes of silver nanoparticles using high-resolution cathodoluminescence spectroscopy, ACS Nano 3 (10) (October 2009) 2965–2974.
[91] L. Gu, W. Sigle, C.T. Koch, J. Nelayah, V. Srot, P.A. van Aken, Mapping of valence energy losses via energy-filtered annular dark-field scanning transmission electron microscopy, Ultramicroscopy 109 (9) (August 2009) 1164–1170.
[92] I.R. Khan, D. Cunningham, S. Lazar, D. Graham, W.E. Smith, D.W. McComb, A tem and electron energy loss spectroscopy (eels) investigation of active and inactive silver particles for surface enhanced resonance raman spectroscopy (serrs), Faraday Discuss. 132 (2006) 171–178.
[93] L. Rodriguez-Lorenzo, R.A. Alvarez-Puebla, I. Pastoriza-Santos, S. Mazzucco, O. Stephan, M. Kociak, L.M. Liz-Marzan, F.J.G. de Abajo, Zeptomol detection through controlled ultrasensitive surface-enhanced raman scattering, J. Am. Chem. Soc. 131 (13) (April 2009) 4616.
[94] P.E. Batson, Surface plasmon coupling in clusters of small spheres, Phys. Rev. Lett. 49 (1982) 936–940.
[95] N. Zabala, A. Rivacoba, P.M. Echenique, Coupling effects in the excitations by an external electron beam near close particles, Phys. Rev. B 56 (12) (September 1997) 7623–7635.
[96] B. Ogut, R. Vogelgesang, W. Sigle, N. Talebi, C.T. Koch, P.A. van Aken, Hybridized metal slit eigenmodes as an illustration of babinet's principle, ACS Nano 5 (8) (August 2011) 6701–6706.
[97] A. Rivacoba, P. Apell, N. Zabala, Energy-loss probability of stem electrons in cylindrical surfaces, Nucl. Instrum. Methods Phys. Res., Sect. B, Beam Interact. Mater. Atoms 96 (3–4) (May 1995) 465–469.
[98] E. Ringe, J.M. McMahon, J.M. McMahon, K. Sohn, C. Cobley, Y. Xia, J. Huang, G. Schatz, L.D. Marks, R.P. VanDuyne, Unraveling the effects of size, composition, and substrate on the localized surface plasmon resonance frequencies of gold and silver nanocubes: A systematic single-particle approach, J. Phys. Chem. C 114 (2010) 12511.
[99] S.P. Zhang, K. Bao, N.J. Halas, H.X. Xu, P. Nordlander, Substrate-induced fano resonances of a plasmonic: Nanocube: A route to increased-sensitivity localized surface plasmon resonance sensors revealed, Nano Lett. 11 (4) (April 2011) 1657–1663.
[100] H. Morkoc, S. Strite, G.B. Gao, M.E. Lin, B. Sverdlov, M. Burns, Large-band-gap SiC, III–V nitride, and II–VI ZnSe-based semiconductor-device technologies, J. Appl. Phys. 76 (3) (August 1994) 1363–1398.
[101] S.J. Xu, S.J. Chua, T. Mei, X.C. Wang, X.H. Zhang, G. Karunasiri, W.J. Fan, C.H. Wang, J. Jiang, S. Wang, X.G. Xie, Characteristics of ingaas quantum dot infrared photodetectors, Appl. Phys. Lett. 73 (21) (November 1998) 3153–3155.
[102] O. Jani, I. Ferguson, C. Honsberg, S. Kurtz, Design and characterization of gan/ingan solar cells, Appl. Phys. Lett. 91 (13) (September 2007) 132117.

[103] N. Gisin, G.G. Ribordy, W. Tittel, H. Zbinden, Quantum cryptography, Rev. Mod. Phys. 74 (1) (January 2002) 145–195.
[104] M. Couillard, M. Kociak, O. Stephan, G.A. Botton, C. Colliex, Multiple-interface coupling effects in local electron-energy-loss measurements of band gap energies, Phys. Rev. B 76 (16) (October 2007) 165131.
[105] B.G. Yacobi, D.B. Holt, Cathodoluminescence Microscopy of Inorganic Solids, Springer US, 1990.
[106] U. Jahn, J. Ristic, E. Calleja, Cathodoluminescence spectroscopy and imaging of GaN/(Al,Ga)N nanocolumns containing quantum disks, Appl. Phys. Lett. 90 (16) (April 2007) 161117.
[107] J. RodriguezViejo, K.F. Jensen, H. Mattoussi, J. Michel, B.O. Dabbousi, M.G. Bawendi, Cathodoluminescence and photoluminescence of highly luminescent CdSe/ZnS quantum dot composites, Appl. Phys. Lett. 70 (16) (April 1997) 2132–2134.
[108] M. Grundmann, J. Christen, N.N. Ledentsov, J. Bohrer, D. Bimberg, S.S. Ruvimov, P. Werner, U. Richter, U. Gosele, J. Heydenreich, V.M. Ustinov, A.Y. Egorov, A.E. Zhukov, P.S. Kopev, Z.I. Alferov, Ultranarrow luminescence lines from single quantum dots, Phys. Rev. Lett. 74 (20) (May 1995) 4043–4046.
[109] J.P. Garayt, J.M. Gerard, F. Enjalbert, L. Ferlazzo, S. Founta, E. Martinez-Guerrero, F. Rol, D. Araujo, R. Cox, B. Daudin, B. Gayral, L.S. Dang, H. Mariette, Study of isolated cubic GaN quantum dots by low-temperature cathodoluminescence, Physica E, Low-Dimens. Syst. Nanostruct. 26 (1–4) (February 2005) 203–206.
[110] L. Rigutti, M. Tchernycheva, A.D. Bugallo, G. Jacopin, F.H. Julien, L.F. Zagonel, K. March, O. Stephan, M. Kociak, R. Songmuang, Ultraviolet photodetector based on GaN/AlN quantum disks in a single nanowire, Nano Lett. 10 (8) (August 2010) 2939–2943.
[111] L. Rigutti, M. Tchernycheva, A.D. Bugallo, G. Jacopin, F.H. Julien, F. Furtmayr, M. Stutzmann, M. Eickhoff, R. Songmuang, F. Fortuna, Photoluminescence polarization properties of single GaN nanowires containing AlxGa(1-x)N/GaN quantum discs, Phys. Rev. B 81 (4) (January 2010) 045411.
[112] J. Renard, R. Songmuang, G. Tourbot, C. Bougerol, B. Daudin, B. Gayral, Evidence for quantum-confined stark effect in GaN/AlN quantum dots in nanowires, Phys. Rev. B 80 (12) (September 2009) 121305.
[113] G. Tourbot, C. Bougerol, F. Glas, L.F. Zagonel, Z. Mahfoud, S. Meuret, P. Gilet, M. Kociak, B. Gayral, B. Daudin, Growth mechanism and properties of ingan insertions in GaN nanowires, Nanotechnology 23 (13) (April 2012) 135703.
[114] L.F. Zagonel, L. Rigutti, M. Tchernycheva, G. Jacopin, R. Songmuang, M. Kociak, Visualizing highly localized luminescence in GaN/AlN heterostructures in nanowires, Nanotechnology 23 (45) (2012) 455205.
[115] R. Paul Edwards, David Sleith, Alastair W. Wark, Robert W. Martin, Mapping localized surface plasmons within silver nanocubes using cathodoluminescence hyperspectral imaging, J. Phys. Chem. C 115 (29) (2011) 14031–14035.
[116] J. Bruckbauer, P.R. Edwards, J. Bai, T. Wang, R.W. Martin, Probing light emission from quantum wells within a single nanorod, Nanotechnology 24 (2013) 365704.
[117] D.A.B. Miller, D.S. Chemla, T.C. Damen, A.C. Gossard, W. Wiegmann, T.H. Wood, C.A. Burrus, Band-edge electroabsorption in quantum well structures – the quantum-confined stark-effect, Phys. Rev. Lett. 53 (22) (1984) 2173–2176.
[118] J. Barjon, J. Brault, B. Daudin, D. Jalabert, B. Sieber, Cathodoluminescence study of carrier diffusion in AlGaN, J. Appl. Phys. 94 (4) (August 2003) 2755–2757.
[119] S.J. Pennycock, A. Howie, Study of single-electron excitations by electron microscopy. II. Cathodoluminescence image contrast from localized energy transfers, Philos. Mag. A 41 (1979) 809–827.
[120] N. Yamamoto, J.C.H. Spence, D. Fathy, Cathodoluminescence and polarization studies from individual dislocations in diamond, Philos. Mag. B 49 (6) (1984) 609–629.
[121] B. Wilsch, U. Jahn, B. Jenichen, J. Lahnemann, H.T. Grahn, H. Wang, H. Yang, Spatially resolved investigation of strain and composition variations in (In,Ga)N/GaN epilayers, Appl. Phys. Lett. 102 (5) (February 2013) 052109.
[122] A. Pierret, C. Bougerol, B. Gayral, M. Kociak, B. Daudin, Probing alloy composition gradient and nanometer-scale carrier localization in single AlGaN nanowires by nanocathodoluminescence, Nanotechnology 24 (2013) 305703.
[123] L.H.G. Tizei, M. Kociak, Spectrally and spatially resolved cathodoluminescence of nanodiamonds: local variations of the NV0 emission properties, Nanotechnology 23 (17) (May 2012) 175702.
[124] W.E. Lamb, Anti-photon, Appl. Phys. B, Lasers Opt. 60 (2–3) (February 1995) 77–84.
[125] A. Beveratos, R. Brouri, T. Gacoin, A. Villing, J.P. Poizat, P. Grangier, Single photon quantum cryptography, Phys. Rev. Lett. 89 (18) (October 2002) 187901.
[126] J. McKeever, A. Boca, A.D. Boozer, R. Miller, J.R. Buck, A. Kuzmich, H.J. Kimble, Deterministic generation of single photons from one atom trapped in a cavity, Science 303 (5666) (March 2004) 1992–1994.
[127] S. Kako, C. Santori, K. Hoshino, S. Gotzinger, Y. Yamamoto, Y. Arakawa, A gallium-nitride single-photon source operating at 200k, Nat. Mater. 5 (11) (November 2006) 887–892.
[128] L.H. Robins, L.P. Cook, E.N. Farabaugh, A. Feldman, Cathodoluminescence of defects in diamond films and particles grown by hot-filament chemical-vapor deposition, Phys. Rev. B 39 (18) (June 1989) 13367–13377.
[129] N. Mizuochi, T. Makino, H. Kato, D. Takeuchi, M. Ogura, H. Okushi, M. Nothaft, P. Neumann, A. Gali, F. Jelezko, J. Wrachtrup, S. Yamasaki, Electrically driven single-photon source at room temperature in diamond, Nat. Photonics 6 (5) (May 2012) 299–303.
[130] A. Lohrmann, S. Pezzagna, I. Dobrinets, P. Spinicelli, V. Jacques, J.F. Roch, J. Meijer, A.M. Zaitsev, Diamond based light-emitting diode for visible single-photon emission at room temperature, Appl. Phys. Lett. 99 (25) (December 2011) 251106.